# Detrital carbonate minerals in Earth's element cycles

**Gerrit Müller*[,a], Janine Börker[b], Appy Sluijs [a], Jack J. Middelburg [a]**

[a] *Department of Earth Sciences, Utrecht University, The Netherlands*

[b] *Institute for Geology, CEN (Center for Earth System Research and Sustainability), Universität Hamburg, Germany*

*g.muller@uu.nl*

*janine.boerker@uni-hamburg.de*

*A.Sluijs@uu.nl*

*J.B.M.Middelburg@uu.nl*

* *corresponding author: Gerrit Müller*

*Mail: g.muller@uu.nl*

Address: Vening Meineszgebouw A, Princetonlaan 8a, 3584 CB Utrecht, The Netherlands

*Abbreviations: PIC: Particulate inorganic carbon, DIC: Dissolved inorganic carbon, POC: Particulate Organic Carbon, DOC: Dissolved Organic Carbon, SOC: Soil organic carbon, TC: Total river carbon, SVM: Support Vector Machine, MGGP: Multi-Gene Genetic Programming, SR: Symbolic Regression, RMSE: Root mean squared error, MC: Monte Carlo, VI: Variable Influence, fwm: flux-weighted mean, med: median, mod: modelled, wo: without, S: related to change in sediment discharge, D: related to damming, SC: Source Carbonate, hdi: human development index, gdp: gross domestic product, nli: night light index, pop: population count.*

# Key points:

- The present day riverine detrital carbonate flux from land to sea is 3.0 ± 0.4 Tmol C/y.
- Associated calcium, alkalinity and strontium contribute significantly to their global biogeochemical cycles.
- Damming reduced the riverine PIC flux by 25 % (from naturally 4.0 ± 0.5 Tmol C/y).

**Abstract.** We investigate if the commonly neglected riverine detrital carbonate fluxes might balance several chemical mass balances of the global ocean. Particulate inorganic carbon (PIC) concentrations in riverine suspended sediments, i.e., carbon contained by these detrital carbonate minerals, was quantified at the basin and global scale. Our approach is based on globally representative datasets of riverine suspended sediment composition, catchment properties and a two-step regression procedure. The present day global riverine PIC flux is estimated at 3.0 ± 0.4 Tmol C/y (13% of total inorganic carbon export and 4 % of total carbon export). The flux prior to damming was 4.0 ± 0.5 Tmol C/y, with a flux-weighted mean concentration is 0.26 ± 0.03 wt%. PIC fluxes are concentrated in limestone-rich, rather dry and mountainous catchments of large rivers in Arabia, South East Asia and Europe with 2.2 Tmol C/y (67.6 %) discharged between 15 °N and 45 °N. Greenlandic and Antarctic meltwater discharge and ice-rafting additionally contribute 0.8 ± 0.3 Tmol C/y. This amount of detrital carbonate minerals annually discharged into the ocean implies a significant contribution of calcium (4.6 Tmol Ca/y) and alkalinity fluxes (9.6 Tmol(eq)/y) to marine mass balances and moderate inputs of strontium (4.8 Gmol Sr/y), based on undisturbed riverine and cryospheric inputs and a dolomite/calcite ratio of 0.1. Magnesium fluxes (0.2 Tmol Mg/y), mostly hosted by less-soluble dolomite, are rather negligible. These unaccounted fluxes help balancing, albeit not completely close, respective marine mass balances and potentially alter any conclusions based on these budgets.

**Plain Language Summary.** Earth surface conditions, including climate and sea level, are largely controlled by the cycling of carbon and biogeochemically coupled elements. However, most elemental budgets cannot be consentaneously balanced for the present state. Here, we investigate the possible role of riverine carbonate minerals in such marine mass balances. We derive individual river basin export fluxes, the global export flux to the ocean and its reduction by human influence, utilizing state-of-the-art regression techniques and published global-scale datasets. Results point to a significance of riverine detrital carbonates for the global mass balances of carbon, calcium, alkalinity and strontium, which might help solving this long-standing problem.

## Graphical Abstract

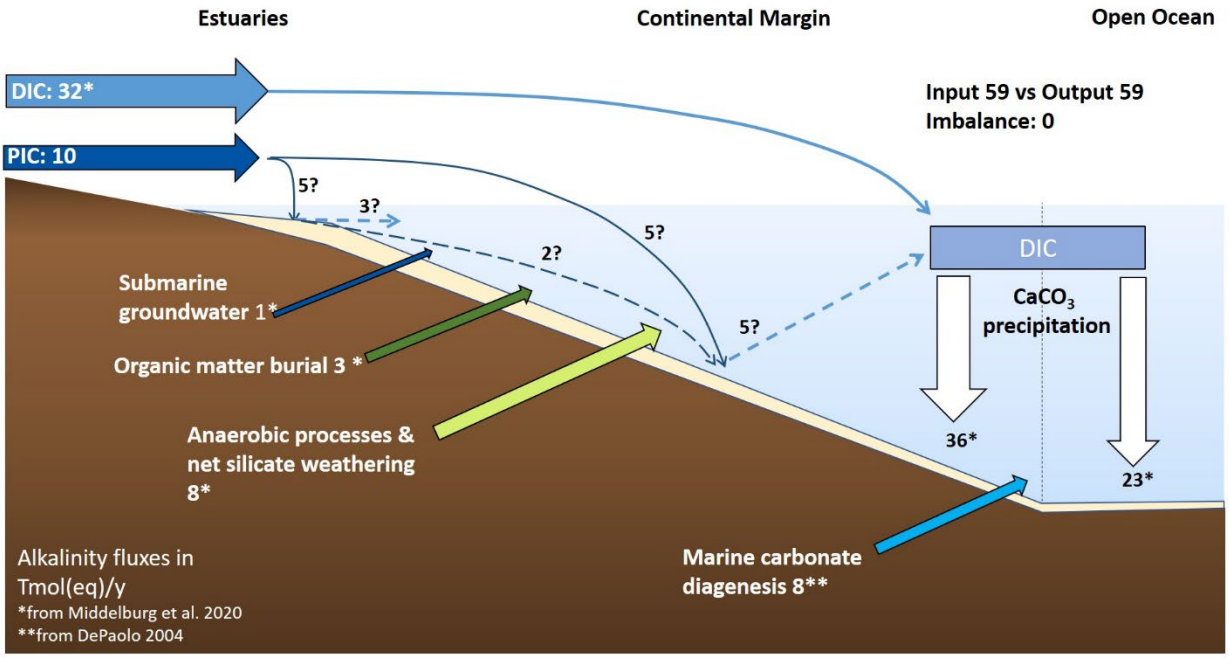

# 1 Introduction

Erosion and weathering of Earth's surface not only shape landscapes, but also influence the global carbon cycle, thereby maintaining the habitability of our planet (Ebelmen, 1845; Urey, 1952; Berner et al., 1983; West et al., 2005; Ferrier and West, 2017; Penman et al., 2020). Oceanic mass balances of carbon (C) and biogeochemically coupled elements provide a powerful tool to investigate these processes and their role in the Earth system globally and over longer time-scales (classically > 100 ka) (Dickens, 2001; Krabbenhöft et al., 2010; Tipper et al., 2010; Berner and Berner, 2012). They also allow quantification of hardly measurable processes, such as global rates of marine carbonate burial or hydrothermal activity (Tipper et al., 2006; van der Ploeg et al., 2019; Shalev et al., 2019). However, some of the most prominent and most frequently considered budgets presented in that context remain unbalanced and/or highly debated, such as that of Ca, Mg, Sr and alkalinity (Berner and Berner, 1987; Milliman, 1993; Gislason et al., 2006; Tipper et al., 2006; Krabbenhöft et al., 2010; Tipper et al., 2010; Berner and Berner, 2012; Jones et al., 2012; Lebrato et al., 2020). This is usually explained by disequilibrium, i.e., the present state strongly differs from average Pleistocene conditions, by proposing a variety of smaller-scale marine processes and/or by invoking yet unaccounted input fluxes (Milliman, 1993; Krabbenhöft et al., 2010; Tipper et al., 2010; Shalev et al., 2019; Middelburg et al., 2020).

For most budgets, riverine dissolved loads are considered the only major input term, reflecting the catchment-integrated result of chemical rock weathering as transported by the Earth-spanning fluvial networks (Berner and Berner, 1987; Berner and Berner, 2012). Some authors recognized submarine groundwater discharge as another important flux to the ocean with a probable magnitude of 0.7 to 6 % of the global river discharge (Milliman, 1993; Zhou et al., 2019; Mayfield et al., 2021). In addition to these dissolved inputs, it is generally accepted that organic and biogenic riverine particles exert major control on the biogeochemical cycling

of carbon (C), nitrogen (N) and phosphorous (P) (Berner, 1982; Froelich et al., 1982; Berner, 1999; Boyer and Howarth, 2008; Hilton and West, 2020), and of silicon (Si) (Conley, 2002; Sutton et al., 2018). Moreover, the importance of ions and complexes sorbed to the surfaces of riverine sediments was highlighted (Berner et al., 1983; Tipper et al., 2021). A similar importance was proposed for particulate inorganic forms (mineral detritus) of silicon (Si) (Mackenzie and Garrels, 1965; Mackenzie and Garrels, 1966), calcium (Ca) (Gislason et al., 2006), strontium (Sr) (Jones et al., 2012; Hong et al., 2020), and iron (Fe) (Poulton and Raiswell, 2002; Luo et al., 2020), based on experimental and field-measured element release rates. Recently, based on a limited dataset, Middelburg et al. (2020) suggested that riverine particulate inorganic carbon (PIC) fluxes to the ocean may be about 1/3 of riverine dissolved inorganic carbon (DIC) fluxes and that the ocean alkalinity budget is close to balance when this is considered an additional alkalinity input. While basaltic minerals and glasses of volcanic origin are currently considered to be the major host minerals of particulate Ca and Sr fluxes (Gislason et al., 2006; Jones et al., 2012; Torres et al., 2020), significant riverine PIC fluxes would imply substantial additional Ca, Sr and Mg delivery in particulate forms.

Carbonate dissolution and recrystallization are well known to occur in estuaries (Aller, 1982; Gattuso et al., 1998; Santos et al., 2019) and the ocean (Milliman, 1974; Krumins et al., 2013; Sulpis et al., 2017), providing evidence for the (partial) release of Ca, Mg, Sr, IC and alkalinity from detrital sources to the oceanic inventories. Dissolution of PIC in the ocean could, thus, represent a major missing term in oceanic mass balances, potentially altering the conclusions deduced from those budgets (e.g., Berner and Berner, 2012; Krabbenhöft et al., 2010; Paytan et al., 2021; Tipper et al., 2006, 2010). Notably, recrystallization within the sediment column, i.e., dissolution and direct re-precipitation, may still result in an exchange of PIC-derived and marine elements and isotopes (DePaolo, 2004; Fantle et al., 2010; Paytan et al., 2021).

High solubility and rapid dissolution kinetics of carbonate minerals cause the dominant mass of IC to be transported in dissolved form (Lasaga, 1984). Therefore, the significance of detrital carbonate minerals in river sediments is often neglected. However, detrital carbonates are commonly observed constituents of suspended sediments in rivers (Mackenzie and Garrels, 1966; Müller et al., 2021a) and even authigenic carbonate production in calcite-saturated rivers is common (Kempe and Emeis, 1985; Négrel and Grosbois, 1999; Grosbois et al., 2001). Sr-isotopic constraints suggest that 30 – 50 % of the carbonate minerals within the Gulf of Lyon sediments are detrital, even more during glacial periods (Pasquier et al., 2019). Additionally, the isotopic composition of carbonates from turbidites in the Bengal fan, one of the largest sediment dispersal systems on earth (Mouyen et al., 2018), suggests a mixture of biogenic (> 85 wt%), detrital (up to 10 wt%) and diagenetic (1.2 – 4 wt%) origin (France-Lanord et al., 2018). This indicates that the PIC delivery may indeed be a relevant flux to the marine realm, but its size and dissolving fraction remain unclear because a global assessment is lacking.

We aim to better constrain these important numbers based on several approaches. First, we establish a first-order calculation based on published average PIC and CaO concentrations and sediment fluxes. Next, we quantify PIC concentrations and fluxes globally at the basin-scale, using published datasets of riverine suspended sediment and catchment characteristics, and a two-step regression procedure, involving regressive classification through Support Vector Machines (SVM) and symbolic regression by multi-gene genetic programming (MGGP). Controlling factors of the global PIC flux, human influence and the fate of the delivered detrital carbonates in the ocean are then discussed, including implications for oceanic mass balances and carbon cycling.

## 2 Methods and procedures

To calculate the global PIC flux, we need a gapless set of PIC concentrations and sediment

fluxes of all rivers in the world. The latter can be generated using advanced models that provide sediment fluxes of global rivers in space and time, based on water balance and catchment properties (WBMSed 2.0, Cohen et al., 2014). These data, along with the locations of the river mouths, were taken from a compilation of the *GlobalDelta* project (Nienhuis et al., 2020). No such model is available for PIC concentrations yet. Hence, we here develop a statistical, spatially-explicit model that predicts PIC concentrations from catchment properties.

Annual median PIC concentrations were calculated for all locations in the GloRiSe v1.1 database (Müller et al., 2021b) from direct measurements, mineralogical and petrographic observations or empirically from major element composition (Supplementary Information SI 1). The uncertainty of these concentrations was defined as the mean relative deviation of single measurements from the flux-weighted mean of available time-series (Müller et al., 2021b). A large set of hydro-environmental and physiographic variables was derived from the HydroBasins database (Linke et al., 2019) by spatially assigning each GloRiSe-location to the corresponding sub-basin (at Pfafstetter level 7). Annual averages for the upstream catchment of nine variables were selected based on correlation analysis and/or a causal link to PIC concentrations (Supplementary Information SI 1). These variables cover topography, vegetation, hydrology, climate and human impact (Table 1). As the carbonate in the catchment is the source of riverine PIC, a proper indication of this 'source carbonate' (SC) was extracted from global maps of lithology (GLiM, Hartmann and Moosdorf, 2012), unconsolidated sediments (GUM, Börker et al., 2018) and soils (WISE, Batjes, 2012). For soils, the carbonate content was given directly, while for each rock and sediment class a global representative estimate of the carbonate content was taken from literature (Supplementary Information SI 1). Area-weighted upstream averages were calculated individually for the carbonate content of GliM, GUM and WISE in each basin. Next, these were summed and normalized to 100 % to represent the SC, i.e., carbonate available to be transported as PIC. All the predictor variables

158 are summarized in Table 1. Catchments with SC < 10 % were assumed to be PIC-free, as
159 dissolution usually dominates over detrital carbonate transport in (undersaturated) rivers (see
160 1 Introduction).

***Table 1*** *Predictor variable selection to model PIC concentrations. Variables are taken from HydroBasins (Linke et al., 2019), except for the potential source carbonate, which was calculated from global soil, sediment and lithological maps* (Batjes, 2012; Hartmann and Moosdorf, 2012; Börker et al., 2018)*. All variables represent the upstream-average of a specific HydroBasins sub-basin at Pfafstetter level 7. Abbreviations: hdi: human development index, gdp: gross domestic product, nli: night light index, pop: population count.*

| Topography & Vegetation | Underground & Humans | Climate & Hydrology |
|---|---|---|
| Elevation | Potential source carbonate (rock, sediment, soil) | Precipitation |
| Upstream catchment area | Soil organic carbon content | Temperature |
| Forestation | Human factor (log(hdi+gdp+nli+pop)) | Extent of water bodies (rivers, lakes, reservoirs) |
| Bare areas (rock, desert, tundra, open shrub land) | | |

161

162 **2.1 Regression & Upscaling**
163

164 To estimate PIC concentrations in the remaining ~65 % of the global suspended sediment
165 discharge, we employed a two-step regression procedure consisting of (I) a qualitative
166 indication of the presence of PIC in a catchment (yes/no) and (II) a quantitative regressive
167 estimation of the PIC concentration. This two-step procedure was necessary because PIC
168 concentrations are not only log-normally distributed, but also frequently close or equal to zero,
169 thus hampering the regression procedure, which is a well-known problem in ecology (Fletcher
170 et al., 2005).

171 For the qualitative model, we applied a Support Vector Machine (SVM), a standard
172 technique from the MATLAB 2019b Machine Learning toolbox. This model was trained and
173 forced by only five variables, because SVMs have been found to achieve better results with

174 less variables (Kitsikoudis et al., 2013). We chose to use SC, precipitation, elevation,
175 forestation and human factor, covering the most diverse aspects of sources and preservation
176 potential of PIC. PIC concentration was assumed not present if it was below 0.1 wt%,
177 approximating the uncertainty of most measurements included in *GloRiSe*. SVM was chosen,
178 because it performed slightly better than alternative methods, such as logistic regression and
179 ensemble techniques.

180 For the quantitative model, symbolic regression (SR) by means of multi-gene genetic
181 programming (MGGP) was used, providing a fully data-driven tool to find both the model
182 structure and its parameters. The implemented SR-algorithm pseudo-randomly creates linear
183 combinations of (potentially non-linear) terms, which are tested and evolved to best fit the
184 observed PIC concentrations as assessed by the root mean squared error (*GPTIPS* 2.0, Searson
185 et al., 2010). Thus, SR is able to cover non-linear relationships between the variables and its
186 performance seems comparable to artificial neural networks, while it still results in comparably
187 simple equations that can be related to the governing processes (Kitsikoudis et al., 2013;
188 Gandomi et al., 2015; Jin et al., 2019). Variable selection and SR intrinsically determine the
189 importance of individual variables for, and their direction of relationship to PIC concentrations,
190 which we quantitatively assess using the linear correlation coefficient and coefficient of
191 determination (R and $R^2$, respectively, at $p < 0.01$) between the median result of 830 accepted
192 Monte Carlo simulations and each variable. This method reduces biases due to multi-
193 collinearity and non-linearity and is commonly applied to the evaluation of canonical
194 correlations analyses (Kuylen and Verhallen, 1981).

195 The global riverine PIC flux is the sum of the products of sediment fluxes and PIC
196 concentrations in each basin draining directly to the coastal ocean. For a proper re-estimation
197 and uncertainty analysis, the regression and prediction procedure was repeated 2,000 times
198 with a (pseudo-)random perturbation of sediment fluxes and PIC concentrations within the

range of their respective uncertainties, including the full model derivation via SVM and SR. The final result is the mean of 830 accepted simulations that produced less than 0.3 % outliers in respect to the 10 % and 90 % percentile (10 of 3364 coastal basins) and its uncertainty is the standard deviation of these models (Koehler et al., 2009). For comparison, we also provide literature-based first-order estimates of riverine PIC fluxes (Supplementary Information S3). Because much less detailed data is available for atmospheric and cryospheric PIC contributions, these fluxes were estimated using published PIC concentrations and sediment fluxes (Supplementary Information S3).

## 3 Results

We calculate that currently 3.1 ± 0.3 Tmol PIC/y are annually discharged to the coastal ocean. The pre-human flux was 4.1 ± 0.5 Tmol PIC/y; the 25 % reduction is caused by particle retention in reservoirs (Fig. 1). The uncertainty of 10 % appears low, considering the much larger uncertainty of sediment fluxes (50 %), observed PIC concentrations (50 %) and

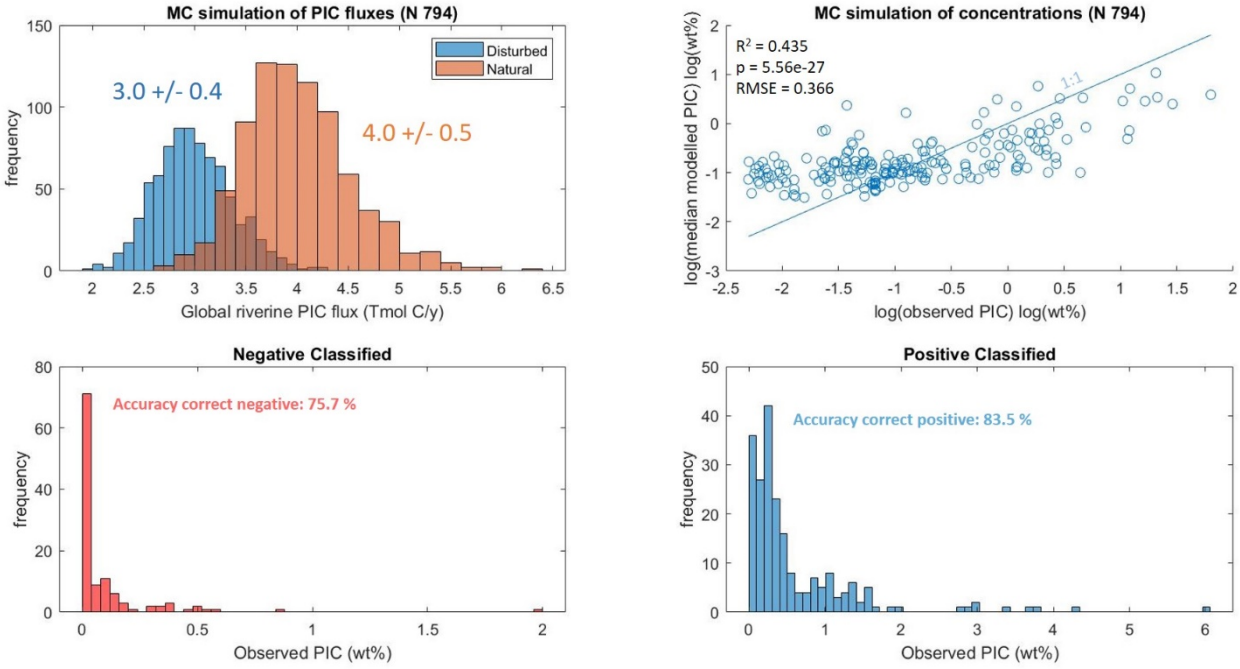


***Figure 1**: Results (upper) and performance (lower) of the Monte Carlo-refined regression procedure. Histograms (upper panels) show the distribution of natural (left) and anthropogenically disturbed (right) global PIC fluxes. The lower panels evidence the performance of an exemplary quantitative model (left, prediction within factor 4) and the qualitative classification (right).*

***Table 2*** *Comparison of the herein presented results and literature-based estimates of global average PIC concentration (cPIC), flux-weighted mean, median and mixture of median and mean, respectively), suspended sediment discharge (fTSS, global sum) and PIC flux (fPIC, global sum). References: 1: Meybeck (1982), 2: Viers et al. (2009), 3: Savenko (2007), 4: Bayon et al. (2015), 5: Beusen et al., (2005), 6: Milliman and Farnsworth (2011), 7: Syvitski and Kettner (2011), 8: Cohen et al. (2014), 9: Middelburg et al. (2020) based on Canfield, (1997) and Beusen et al. (2005), 10: Meybeck (1993), 11: Journet et al. (2014), 12: Jickells et al (2005), 13: Overeem et al. (2017), 14: Raiswell et al. (2008), 15: Wadham et al. (2013). Abbreviations: med: median, fwm: flux-weighted mean, obs: observations, wo: without, $Q_s^{nat}$: natural sediment discharge. 'Literature' indicates values and ranges that were calculated from published values ('first-order' estimates (Supplementary Information SI 2, grey columns). 'This study' refers to values we derived in this contribution (2 Methods & Procedures, Supplementary Information SI 1). Bold numbers indicate the values suggested for further use.*

| **Variable (unit)** | **cPIC (wt%)** | **cPIC (wt%)** | **cPIC (wt%)** | **fTSS river (Gt/y)** | **fPIC river, $Q_s^{nat}$ (Tmol C/y)** | **fPIC river, actual (Tmol C/y)** | **fPIC river, actual (Tmol C/y)** | **fPIC atmosphere (Tmol C/y)** | **fPIC cryosphere (Tmol C/y)** |
|---|---|---|---|---|---|---|---|---|---|
| **Value** | **0.26** | 0.42 | 0.7 | 16 | **4.1** | **3.1** | 10.4 | **0.25** | **0.78** |
| **Range** | **0.24 – 0.28** | 0.1 – 0.7 | 0.4 - 1 | 12 - 20 | **3.6 – 4.6** | **2.8 – 3.4** | 4.0 – 16.7 | **0.10 – 0.40** | **0.48 – 1.12** |
| **Reference** | This study (fwm, model) | This study (med, obs.) | Literature (1 – 4) | Literature (5-8) | This study (model) | This study (model) | Literature (1 – 10) | Literature (11,12) | Literature (13-15) |

quantitatively modelled PIC concentrations (factor 4) (Supplementary Information S2.3). The reason is the low uncertainty of PIC presence: correct negative classifications (75.7 %) have a lower range of 0 – 0.1 wt% and basins with less than 10 % source carbonate are assumed to have a PIC concentration and error of 0 wt%. Positive classifications are similarly accurate (83.5 %). However, these uncertainties do not account for inaccuracies in the input datasets.

For instance, the global lithological map (*GLiM*) has an accuracy of only ~ 60% compared to point observations (Hartmann and Moosdorf, 2012). The flux-weighted mean PIC

concentration of 0.26 ± 0.03 wt% is lower than the median of PIC-bearing rivers only (0.41 ± 0.01 wt%, excluding PIC-free rivers) implying ~40 % of the riverine sediment flux to be PIC-free. Both are statistically indistinguishable from the median of observed basinal averages (0.35 ± 0.3 wt%), covering ~ 35 % of the global sediment flux (Cohen et al., 2014). Additionally, some authors used mean values, which are more susceptible to outliers caused by small rivers and are typically higher than medians (because of log-normal distributions). High PIC concentrations are rarely found in rivers with high discharge, except for a few large rivers draining markedly dry (e.g., the Nile and Euphrates-Tigris systems) and/or mountainous (e.g., the Indus system) catchments (Fig. 3).

From a total of 3365 catchments considered, the biggest 862 basins contribute ~ 99 % of the total PIC flux, while the biggest 10 catchments, situated in South-East Asia, Arabia, Europe and North America already sum up to ~ 53 %. The Euphrates-Tigris system (13.3 %), the Indus (10.3 %) and the Nile (8.9 %) alone contribute 32.6 % of the total global PIC flux, followed by Yangtze (4.5 %), Salween (4.4%), Colorado (USA, 3.4 %), Rhone (2.8 %),

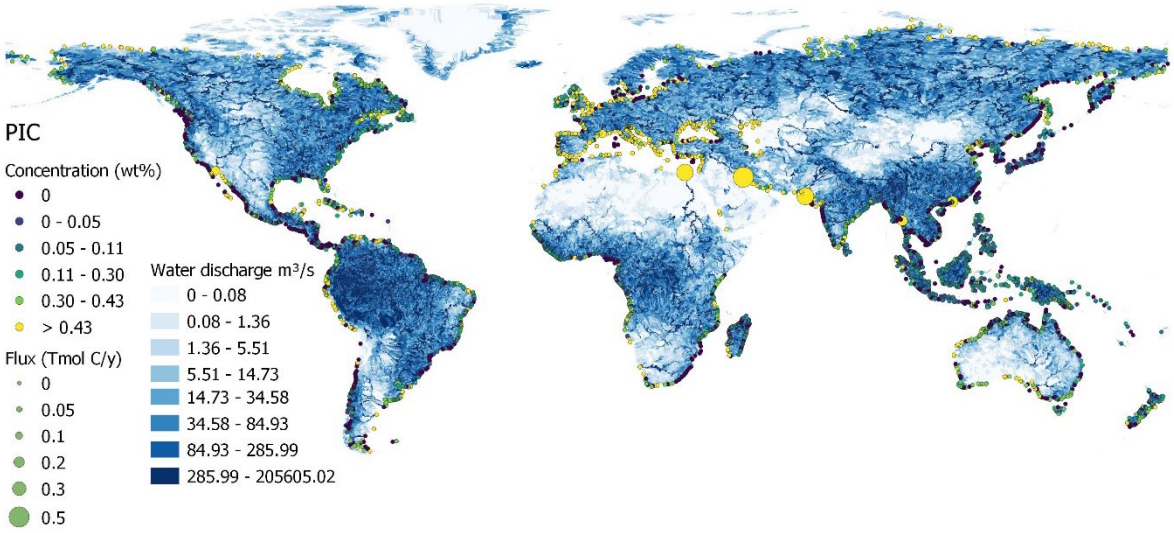


***Figure 1*** *Map of the model results. Point data along the coast are the result of this study (Mean of 3000 Monte Carlo simulations). Size scales with the magnitude of the PIC flux (Tmol C/y), based on natural sediment discharge) and color is related to PIC concentration (wt %). For comparison, blue colors indicate natural annual mean water discharge ($m^3/s$) (Linke et al., 2019)*

234 Huanghe (2.1 %), Mississippi (2.0 %) and the Ganga-Brahmaputra system (1.6 %). 2.7 Tmol
235 PIC/y (67.6 %) is delivered to the coastal ocean between 15 °N and 45 °N, contrasting riverine
236 DIC, OC, total solute and bulk sediment fluxes (Ludwig et al., 1996; Milliman and Farnsworth,
237 2011; Hartmann et al., 2014). The anthropogenic reduction of the global PIC flux is dominated
238 by the decreasing contribution of the Nile due to intense damming (~ 8 of 25 %).

239 The present PIC flux related to atmospheric dust deposition is 0.25 ± 0.15 Tmol C/y,
240 which is ~ 3 % of the riverine PIC flux and ~ 0.3 % of the total riverine carbon flux (~ 71 Tmol
241 C/y, Supplementary Information S3). Thus, the atmospheric contribution is negligible in global
242 mass balances. PIC related to meltwater discharge and ice-rafted debris from Greenland and
243 Antarctica together contribute another 0.8 ± 0.3 Tmol PIC/y, which is ~ 26 % of the present
244 day riverine PIC flux and ~ 1 % of the total river carbon flux (Supplementary Information S3).
245 In total, ~ 4 Tmol PIC arrive in the ocean annually.

246 # 4 Discussion

247 ## 4.1 Natural controls of PIC and their variation through time

The relevance of each variable to the model was assessed through the coefficients of correlation and of determination between the individual variable and the median model outcome, being independent of non-linearity and multi-collinearity (Fig. 3). A strong positive influence of SC on PIC concentrations is eminent from these procedures (+ 38 %, Fig. 3). SC includes carbonate from soils (~ 3 % on average) and unconsolidated sediments (~ 2 – 4 %) but is dominated by lithological (bedrock) contributions (~ 20 % on average). This is because terrestrial carbonate weathering is dissolution-dominated, which arises from fast dissolution rates and high solubility (Lasaga, 1984; Morse and Arvidson, 2002). This contrasts with the precipitation-dominated behavior of silicates, producing clay minerals and oxides characteristic to soil assemblages (Lasaga, 1984; Morse and Arvidson, 2002; Brantley et al., 2008; Ma et al., 2011).

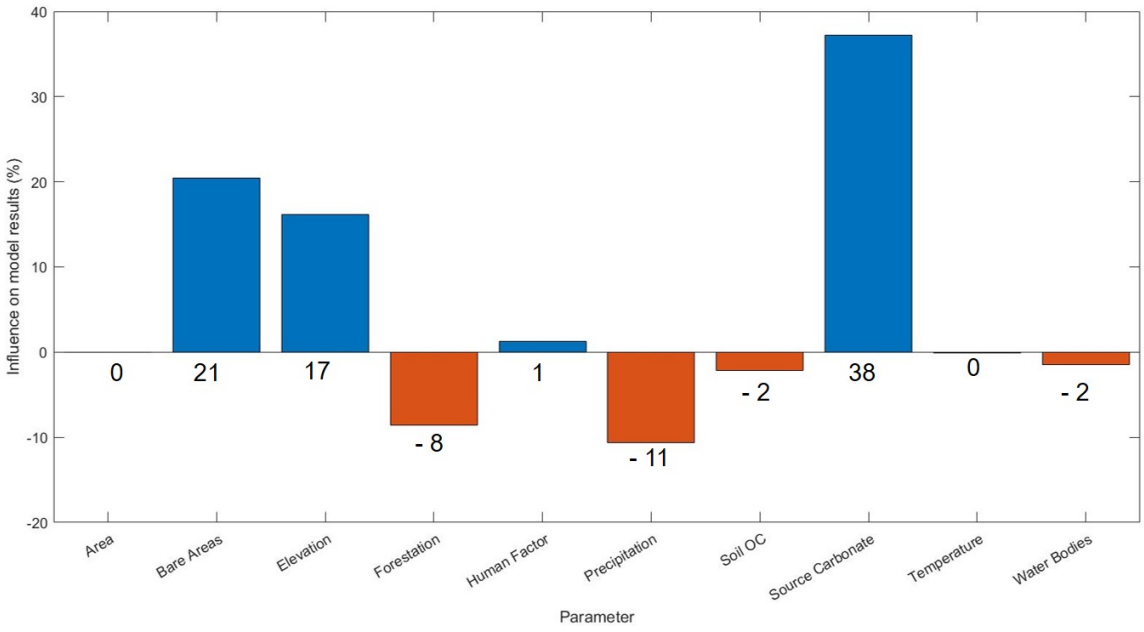


***Figure 3*** *Relative importance of the different variables to our model results as assessed by the coefficient of determination ($R^2$) between the variable in question and the median result of 794 high-quality Monte Carlo simulations. The correlation coefficient gives the direction of influence (orange: negative, blue: positive). Individual values are indicated above the bars. OC: Organic Carbon. Variables correspond to (Table 1).*

Generally, riverine suspended sediment is a mixture of source rocks, their solid weathering products (soil and sediment), organic matter and material of anthropogenic origin, with additional in-stream processing. Thus, the differences between SC and PIC may arise from preferential dissolution of carbonates compared to silicates in the weathering zone (= soil) before erosion, and also from in-stream dissolution (Dornblaser and Striegl, 2009), precipitation (e.g., Kempe and Emeis, 1985; Négrel and Grosbois, 1999) and particle sorting during transport (e.g., Bouchez et al., 2011; Garzanti et al., 2011). According to our results, humans did not significantly influence riverine PIC concentrations on a global scale (yet; Fig. 3), in contrast to sediment fluxes (see section 4.2 Human activities and riverine carbon).A thick soil cover can only develop if chemical weathering rates exceed material removal by erosion (West, 2012; Ferrier and West, 2017), and it is promoted by biological activity. Especially forestation stabilizes the soil, disintegrates pristine rocks and introduces organic acids and

ligands, increasing mineral solubilities (Calmels et al., 2014; Brantley et al., 2017).

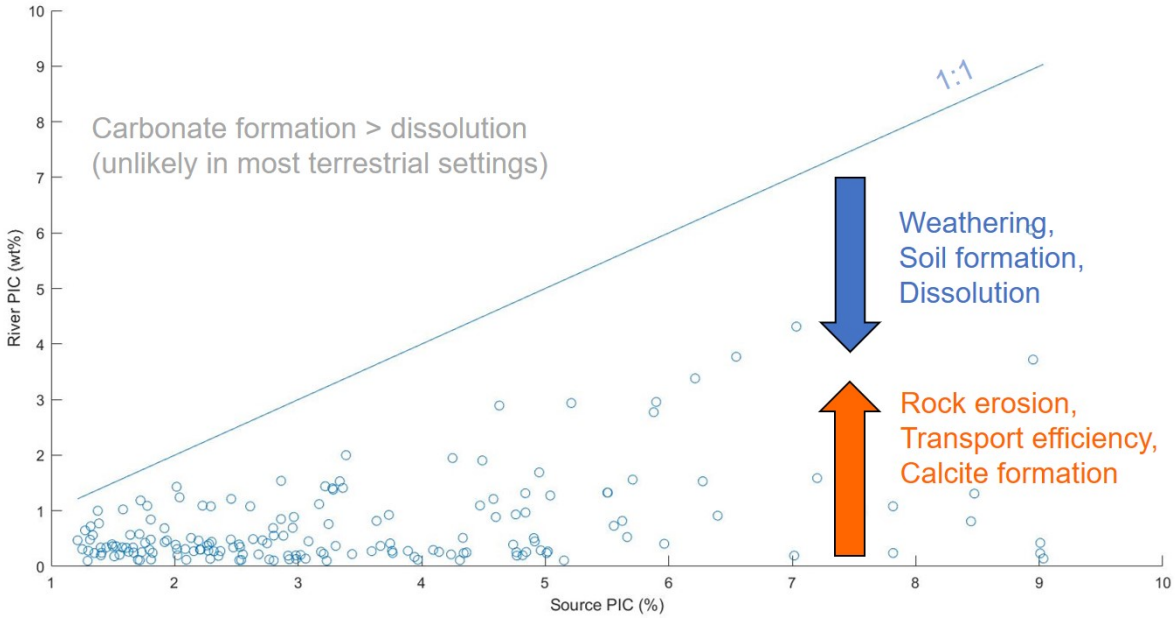


***Figure 4*** *Relationship of river PIC and source PIC. Source PIC (12 % of SC) includes sediment and soil contributions but is dominated by rocks. In-stream dissolution and contributions of weathered material decrease river PIC, while rock erosion has a pronounced positive effect by contributing source rock. Transport efficiency and in-stream precipitation can further enhance PIC concentrations at the river mouth.*

This view is supported by the negative impact of variables in favor of soil formation and dissolution, such as precipitation (- 11 %) and forestation (- 8 %). In contrast, the organic carbon content of soils and temperature, which may influence dissolution kinetics, do not seem to play a major role for PIC concentrations, nor do catchment size or the extent of water bodies, (relatable to the residence time of the particles within the fluvial system). The more prominent influence of (rock) erosion on PIC concentrations is evident from the large influence of related variables, namely, elevation (+ 17 %) and the extent of bare areas (+ 21 %). Rapidly eroding, mountainous terrains are characterized by fast, efficient transport and diminutive sediment storage (Milliman and Syvitski, 1992; Hilton and West, 2020), limiting both the extent of soil formation (Jenny, 1941; Dixon and von Blanckenburg, 2012) and in-stream dissolution.

248 This interpretation that PIC concentrations increase with erosion is apparently
249 inconsistent with increasing carbonate dissolution following pyrite oxidation and sulfuric acid

production upon accelerated erosion as observed in shale-dominated terrains (Calmels et al., 2007; Torres et al., 2014; Bufe et al., 2021). However, we do not only consider shale-rich, but all carbonate-bearing (> 10 %) terrains in this analysis, which could obscure such relationships. Such an apparent inconsistency was noted for other global scale compilations as well (Bufe et al., 2021). Moreover, PIC is predominantly produced by the physical disintegration of pristine rocks and soils, while this same process promotes dissolution and oxidation kinetics. Thus, trends in PIC concentrations and carbonate dissolution do not strictly oppose each other but may even covary in rapidly eroding terrains.

In summary, the rather slowly changing ($10^3$ – $10^5$ y) tectonic, physiographic and lithological settings seem to exert a dominant control on PIC concentrations as demonstrated by the eminent role of SC and elevation in our model. Superimposed on this base-line situation, much faster variations in climatic and vegetation patterns seem to affect the relative contributions of weathered, PIC-poor soil and pristine, PIC-rich source rock.

Although heavily discussed (Foster and Vance, 2006; Willenbring and Von Blanckenburg, 2010; Caves Rugenstein et al., 2019), many observations suggest that soil formation and/or chemical weathering decreased during cold, dry periods (Jenny, 1941; Berner et al., 1983; Dixon et al., 2016; Schachtman et al., 2019), potentially increasing the ratio of pristine source rock to weathered soil in suspended sediments, thus, the riverine PIC flux. Moreover, glacial activity during cooler periods may accelerate erosion, thus, PIC production and potentially preservation (because of decreased residence times). This is supported by an increase of the detrital carbonate fraction in glacial sediments of the Gulf of Lyon, compared to sediments deposited during interglacial periods (Pasquier et al., 2019). An indication of increased cryogenic PIC deposition in response to ice-sheet dynamics is provided by the so-called ‘Heinrich-events’, which are unusual accumulations of coarse carbonate-rich detritus in marine sediment (Bond and Lotti, 1995; White et al., 2016). In contrast, melting permafrost

exposes old, but fresh organic matter that is rapidly respired (e.g., Walz et al., 2017), potentially increasing PIC dissolution (Aller, 1982; Archer et al., 1989; Oelkers et al., 2011; Calmels et al., 2014). Consistently, although not solely related to carbonate weathering, an increased riverine export of alkalinity in response to the recent warming was reported from large Russian Arctic rivers (Drake et al., 2018).

However, recent observations and theories challenge this simple view (Foster and Vance, 2006; Willenbring and Von Blanckenburg, 2010; Caves Rugenstein et al., 2019), implying more complex and transitional spatio-temporal dynamics of erosion (Foreman et al., 2012; Chen et al., 2018; van de Schootbrugge et al., 2020) and carbonate weathering (Gaillardet et al., 2019; Zeng et al., 2019) and, consequently, of riverine inorganic carbon export. Additionally, environmental conditions and, consequently, carbonate dissolution in the (coastal) ocean are expected to change over multiple time-scales, ranging from seasons and decades (Cai et al., 2011; Wallace et al., 2014) to geological time-scales (Broecker, 1982; Ganeshram et al., 2000; Sluijs et al., 2013), with implications for the magnitude and timing of contribution of PIC to oceanic inventories.

### 4.2 Human activities and riverine carbon

Rivers annually deliver about 31.5 Tmol DIC, 19.1 Tmol DOC and 17.4 Tmol POC to the ocean (Table 3). Including 3.0 Tmol PIC/y increases the total riverine carbon export (TC) to 71.0 Tmol C/y, equating a contribution of 4 %, which is within the uncertainty of the estimates excluding PIC (Table 3). An accurate and precise knowledge of the riverine carbon export is necessary to understand the distribution and fate of anthropogenic carbon perturbations (Resplandy et al., 2018; Friedlingstein et al., 2020). Over the past century these riverine carbon fluxes have changed and continue doing so, likely in response to climate change and local human activities, such as industrialization, changes in land-use, hydrology and agricultural

practices (Lambert et al., 2017; Noacco et al., 2017; Drake et al., 2018; Raymond and Hamilton, 2018; Li et al., 2019; Zeng et al., 2019; Liu et al., 2020).

The net effect of human activity on riverine sediment discharge is a ~10 % reduction, dominated by damming (Syvitski et al., 2005; Cohen et al., 2014), resulting in an even higher reduction of riverine PIC (~ 25 %, Table 3) and OC fluxes (~ 13 %, Maavara et al. (2017)). The differences between those fractions are related to the non-even spatial patterns of riverine carbon discharge (Ludwig et al., 1996; Milliman and Farnsworth, 2011, Figure 2). Damming also increases the residence time of particles in the riverine realm (Rueda et al., 2006), where PIC and POC are commonly remobilized by dissolution/degradation. However, organic matter degradation and burial in reservoirs is very heterogeneous and dependent on reservoir age (Maavara et al., 2017). Low importance for the model (- 2 % for water bodies) indicate a rather negligible effect of reservoirs on PIC concentrations on the global scale. Our human factor is not an important predictor in the model (1 %), despite the expected influence of lime-fertilizers (Haynes and Naidu, 1998; Shoghi Kalkhoran et al., 2019; Zeng et al., 2019), cementitious construction materials (Horvath, 2004), and human-induced soil erosion, affecting the active weathering zone (Govers et al., 2014). PIC could also be reduced by increasing dissolution through industrial or agricultural acids (Wicks and Groves, 1993; Webb and Sasowsky, 1994; Perrin et al., 2008). Eventually, the lack of resolution between those positive and negative influences in our human factor obscures a clearer relationship. Thus, more detailed studies on the different human influences on riverine carbonate are required. Notably, the human influence is correlated to observed PIC concentrations, but this spurious relationship stems from collinearity of SC and human population, both being high in southeast Asia, Europe and North America, confirming our method is correcting for multi-collinearity.

A 25 % reduction of PIC fluxes equates to only 1.4 % of the total riverine carbon flux (TC). The damming-related decrease in organic carbon fluxes (13 % of OC, Maavara et al.

(2017)) results in another 6 % reduction of TC. In contrast, carbonate dissolution-related DIC fluxes likely increase(d) by ~ 13.5 % in the period 1950 – 2100 as a consequence of climate-change and land-use change (Zeng et al., 2019). Such an increase of DIC fluxes would result in a 5.6 % increase of TC, partially compensating the reduction of OC and PIC in terms of total carbon export (total disturbance: - 2 %). This is consistent with the estimation of a somewhat stable riverine TC export as a result of in-stream removal of anthropogenic carbon by POC deposition and respiration (Cole et al., 2007; Regnier et al., 2013).

The bulk anthropogenic effect on total global riverine DIC fluxes remains elusive (Raymond and Hamilton, 2018) and human activities other than dam-building impact terrestrial and freshwater carbon cycling. Notably, humans also change conditions at the site of riverine PIC deposition: The current coastal ocean acidification in response to anthropogenic emissions and eutrophication (Borges and Gypens, 2010; Carstensen and Duarte, 2019) , could enhance PIC dissolution, acting as a heterogeneous buffer (Middelburg et al., 2020).

***Table 3*** *Summary of the riverine carbon export (in Tmol C/y). DIC: (Amiotte Suchet et al. (2003); Gaillardet et al. (1999); Hartmann et al. (2014); Li et al. (2017); Ludwig et al. (1996, 1998); Meybeck (1982), DOC: (Aitkenhead and McDowell (2000); Dai et al. (2012); Harrison et al. (2005); Li et al. (2019); Ludwig et al. (1996, 1998), POC: Beusen et al. (2005); Galy et al. (2015); Li et al. (2017); Ludwig et al. (1996, 1998); Meybeck (1982), Superscripts:* $^{S}$*: By changes in sediment flux only,* $^{D}$*: By damming only (Maavara et al., 2017; This study);* $^{*}$*: By climate change and land-use change for carbonate weathering only (Zeng et al., 2019). Human disturbance of TC is the bulk effect as indicated for DIC, PIC, DOC and POC. 'Literature' indicates averages and ranges taken from the above mentioned studies (grey columns). TC represents the sum of our PIC estimate and DIC, DOC and POC estimates from literature.*

| | **DIC** | **PIC** | **DOC** | **POC** | **TC** |
|---|---|---|---|---|---|
| **Modern global river export (Tmol C/y)** | 31.5 | 3.0 | 19.1 | 17.4 | 71.0 |
| **Percentage of TC** | 44.4 | 4.2 | 26.9 | 24.5 | 100 |
| **Range (Tmol C/y)** | 26.6 - 36.3 | 2.6 - 3.4 | 14.2 - 30.0 | 14.2 - 20.0 | 64.8 - 89.0 |
| **Human disturbance (%)** | +13.5$^{*}$ | -24$^{S}$ | -13$^{D}$ | -13$^{D}$ | - 2 |

| | | | | | |
|---|---|---|---|---|---|
| **Range (%)** | +9.8 - +17.1 | - 8.3 - - 39 | -12.8 - -13.2 | -12.8 - -13.2 | - 2 - + 0.5 |
| **Source** | Literature | This study | Literature | Literature | This study & Literature |

337 However, the bulk anthropogenic effect on total global riverine DIC fluxes remains
338 elusive (Raymond and Hamilton, 2018) and human activities other than dam-building impact
339 terrestrial and freshwater carbon cycling. Notably, humans also change conditions at the site of
340 riverine PIC deposition: The current coastal ocean acidification in response to anthropogenic
341 emissions and eutrophication (Borges and Gypens, 2010; Carstensen and Duarte, 2019) , could
342 enhance PIC dissolution, acting as a heterogeneous buffer (Middelburg et al., 2020).

343 **4.3 Implications for oceanic mass balances**

344 The fate of the detrital carbonate flux in the marine realm, i.e., PIC burial or dissolution,
345 determines the implication of the global PIC flux for oceanic mass balances (Middelburg et al.,
346 2020). PIC preservation may affect global estimates of marine carbonate burial, while PIC
347 dissolution would translate to an additional input of Ca, Mg, Sr, C and alkalinity to the marine
348 solute inventories. Because the scientific community lacks a reliable global quantification of
349 these aspects, we discuss the following questions:

350 1. Where is river PIC deposited?

351 2. Does PIC deposition influence global estimates of carbonate burial?

352 3. Does PIC dissolve and alter oceanic mass balances of Ca, Mg, C, Sr and alkalinity?

353 1. On time scales of years to centuries, a major fraction of the riverine suspended matter
354 remains in the estuary (often ~ 40 - 60 %), while the rest is deposited along the shelves and
355 continental slopes (Meade, 1972; Wright and Nittrouer, 1995). Very narrow shelf
356 morphologies, effective transport along canyons in the slope and large flood events cause minor
357 fractions of the suspended sediment to enter open ocean (Dyer, 1995). Moreover, global sea

358 level fall under cooler climates (average Pleistocene state) exposes the PIC-rich shelf to
359 erosion, shifting depocenters to the slope, where PIC may be further transported to and/or
360 dissolved in the open ocean (Kump and Alley, 1994; Filippelli et al., 2007; Tsandev et al.,
361 2010). Thus, on larger time-scales (>$10^3$ years), most of the riverine PIC that does not dissolve
362 on short time-scale (1 to $10^2$ years) will be transported to the slope (Figure 4). A significant
363 fraction may, however, have dissolved before re-mobilization or remain at the initial site of
364 deposition (preservation of the former estuary/shelf). Saderne et al., (2019) emphasize that
365 some coastal ecosystems, such as mangrove forests and seagrass meadows, efficiently trap and
366 dissolve such detrital carbonate from external sources.

367 2. Riverine PIC burial on the shelves may be implicitly included in carbonate mass
368 accumulation (CMA) rate estimates derived from carbonate content, density and sediment
369 accumulation rates, although microscopic criteria were established to distinguish biogenic and
370 detrital carbonates (Milliman, 1974). However, hot spots of carbonate burial do generally not
371 coincide very well with hot spots of riverine suspended sediment deposition (i.e., carbonate-
372 poor shelves) (O'Mara and Dunne, 2019). Moreover, the dissolving PIC fraction and the
373 fraction that remains at the initial site of deposition (i.e., is not re-eroded from the former
374 estuary over longer time-scales) does not contribute to estimates of carbonate burial on the
375 slope. Therefore, we believe that the effect of riverine PIC deposition on CMA-derived
376 estimates of biogenic carbonate burial is rather limited. In contrast, carbonate burial estimates
377 derived from mass balances (e.g., van der Ploeg et al., 2019) or solution chemistry (e.g., Chung
378 et al., 2003) are directly affected by PIC dissolution.

379 3. Marine surface waters are supersaturated with respect to most carbonate minerals
380 (Peterson, 1966; Milliman, 1974). Therefore, provision of carbonate mineral surfaces by PIC
381 discharge, energetically favoring nucleation of these same minerals, may trigger inorganic
382 carbonate precipitation in the water column (Wurgaft et al., 2016). TIC/TOC ratios of

sediments from the Huanghe estuary, China (Gu et al., 2009; Yu et al., 2018), and trends in alkalinity/DIC ratios in the marginal Red Sea support this view (Wurgaft et al., 2016). Compared to marine carbonate compensation, PIC will rapidly settle in the shallow coastal ocean and the degree of carbonate saturation varies with depth and across different local environments at the seafloor (Aller, 1982; Boudreau and Canfield, 1993). As chemical conditions, especially pH, vary within the sediment column, carbonate may even be dissolved in the upper parts of the sediment column, but formed in the lower, more alkaline parts (Aller, 1994).

Carbonate dissolution at the sediment-water interface and in diagenetic settings is well known (Aller, 1982; Archer et al., 1989; Sulpis et al., 2017). In these settings, aerobic degradation of organic matter may drive carbonate dissolution via the production of $CO_2$ and other acidic compounds (Aller, 1982; Oelkers et al., 2011). Anaerobic degradation produces reduced metabolites such as ammonium, sulfide and iron(II), most of which form strong acids upon upward migration and subsequent re-oxidation in the bioturbated zone, which drastically reduces carbonate saturation (Boudreau and Canfield, 1993; Aller, 1994) and may alter the carbon cycle-coupling of subsequent dissolution (Beaulieu et al., 2011; Huang et al., 2017; Torres et al., 2017; Liu et al., 2018).

Carbonate dissolution may also be influenced by biological activity such as seagrass root oxygen loss, sponge boring and bioturbation (Burdige et al., 2008; Mackenzie and Andersson, 2011; Saderne et al., 2019). Substantial riverine PIC dissolution was observed in the maximum turbidity zone of the eutrophic Loire estuary, France (Abril et al., 2003). Moreover, (detrital) carbonate dissolution driven by eutrophication-related bottom water acidification was observed in the Gulf of St. Lawrence, Canada (Nesbitt and Mucci, 2021) and in the Chesapeake Bay, USA (Shen et al., 2019). The proposed total flux of ~ 4.9 Tmol PIC/y corresponds to 9.8 Tmol(eq)/a of alkalinity (~ 30 % of dissolved equivalent), which is ~ 30 %

lower than the estimate of Middelburg et al. (2020). Despite integration of groundwater discharge, marine organic matter burial, anaerobic processes and marine silicate weathering, the modern ocean alkalinity budget is marked by an imbalance of ~25 % of the output by carbonate burial (59 Tmol(eq)/y in the coastal and open ocean). Half of this imbalance can be closed by inclusion of riverine PIC fluxes, assuming terrestrial PIC will either dissolve or biases estimates of carbonate burial (Graphical Abstract). Part of the residual imbalance could be attributed to other diagenetic processes in the coastal zone, such as marine alumo-silicates weathering (Gislason et al., 2006; Jones et al., 2012; Hong et al., 2020; Torres et al., 2020) and carbonate diagenesis (DePaolo, 2004; Fantle et al., 2010; Paytan et al., 2021). However, part of the imbalance could be real, considering that the residence time of carbonate ions in the ocean (~ 100 ky) is larger then the time since the last glaciation (Milliman, 1993; Middelburg et al., 2020).

The inputs of 4.9 Tmol PIC/y (rivers + cryosphere) further imply ~4.6 Tmol Ca/y, ~0.2 Tmol Mg/y and ~4.8 Gmol Sr/y, assuming ideal stoichiometry, 10 % dolomite (typical value in *GloRiSe* v1.1) and 1000 ppm Sr in calcite and dolomite. This equates to ~34.0 % (Ca), ~4.3 % (Mg) and ~8.8 % (Sr) of the respective dissolved equivalents, representing the current major input terms of the respective marine mass balances (Tipper et al., 2006; Krabbenhöft et al., 2010; Tipper et al., 2010; Berner and Berner, 2012; Mayfield et al., 2021). As dolomites typically exhibit much lower dissolution rates than calcites (Pokrovsky et al., 2005), Mg addition by PIC dissolution is probably even smaller and thus negligible. So far, none of these highly discussed budgets could be consensually balanced, neither at the present state nor in reconstructions of the past – a conundrum persisting already for decades (Berner and Berner, 1987; Milliman, 1993; Tipper et al., 2006; Krabbenhöft et al., 2010; Tipper et al., 2010; Berner and Berner, 2012; Jones et al., 2012; Shalev et al., 2019; Hong et al., 2020; Middelburg et al., 2020; Mayfield et al., 2021).

Riverine PIC input also impacts the Ca-cycle (Figure 5). Apart from riverine dissolved Ca fluxes, submarine groundwater discharge (1 Tmol Ca/yr, Mayfield et al., 2021) and hydrothermal processes (2 - 3 Tmol Ca/yr, DePaolo, 2004) were invoked to balance the high output fluxes by carbonate burial, but still leave an imbalane of 36 %, that can be reduced by further 16 % through consideration of PIC fluxes. The remaining 20 % could be attributed to submarine weathering of volcanogenic silicate debris (Gislason et al., 2006; Jones et al., 2012; Hong et al., 2020; Torres et al., 2020) and/or carbonate diagenesis (3 - 5 Tmol Ca/yr, DePaolo, 2004; Fantle et al., 2010). However, carbonate precipitation in early diagenetic settings would rather represent an additional sink of ~ 1 Tmol Ca/yr and ~ 2 Tmol(eq)/y of alkalinity (Schrag, 2013; Torres et al., 2020).

The fraction of detrital carbonates in coastal margin sediments was estimated to <10 and 50 % in the Bengal fan (France-Lanord et al., 2018) and in the Gulf of Lyon (Pasquier et al., 2019), respectively. If the long-term biogenic carbonate burial on the slope is ~2 Tmol C/y (Milliman, 1993) and all riverine PIC (natural: 4.1 Tmol C/y) either dissolves or is transported

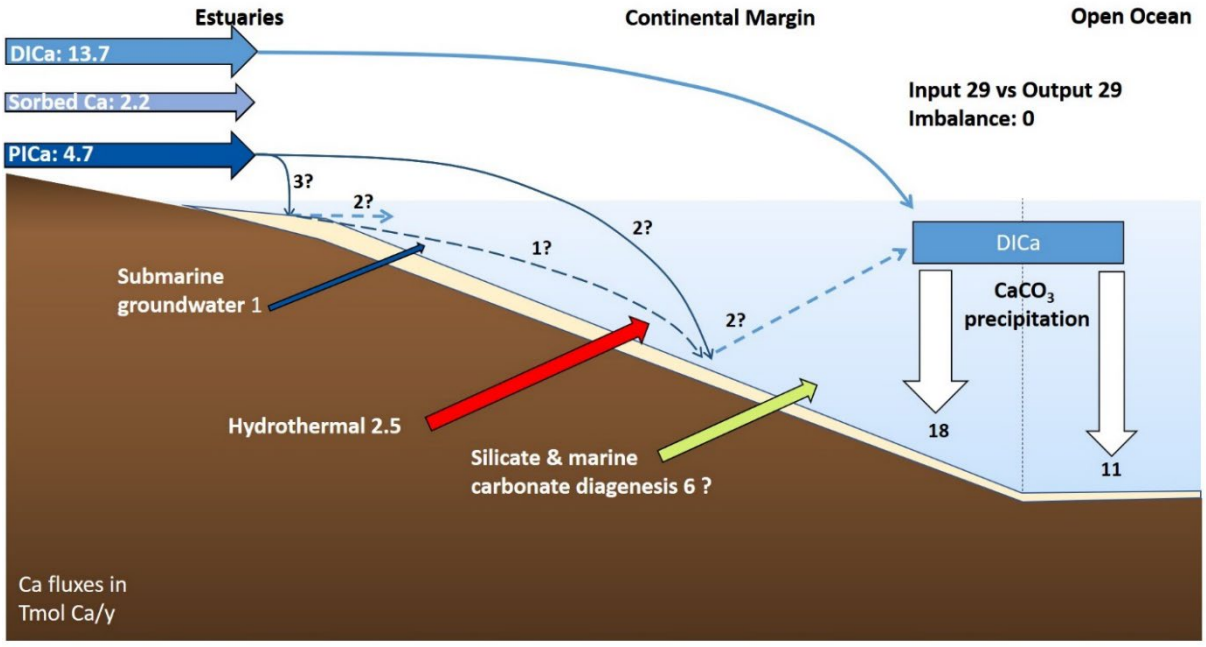


***Figure 4*** *Illustration of the modern ocean calcium budget and how it may be complemented by the inclusion of the riverine PICa flux. The fate of PICa (particulate Ca) in the ocean is,*

*however, uncertain (details in the main text). Fluxes are given in Tmol Ca/y. $CaCO_3$ burial fluxes are from Middelburg et al. (2020), Milliman (1993) and O'Mara and Dunne (2019). River sorbed Ca is from Müller et al., (2021), DICa (dissolved Calcium) and groundwater inputs are from Mayfield et al. (2021), the hydrothermal flux and marine carbonate diagenesis (3 – 4 Tmol Ca/yr)is from DePaolo (2004). The silicate diagenesis flux of Ca is assumed to fill the residual imbalance of ~ 2 Tmol Ca/yr.*

to the slope on long time-scales, then 2.1 to 3.9 Tmol PIC/y (51 – 95 %) would need to dissolve in order to match these detrital fractions. This back-of-the-envelop calculation is not a valid quantification of the globally dissolving PIC fraction, but illustrates PIC dissolution may indeed be significant. However, as argued above, the coastal ocean is a heterogeneous region with locally very spatio-temporally variable conditions supporting carbonate dissolution, preservation as well as precipitation. Importantly, recrystallization still leads to an exchange with the marine element and isotope inventories (e.g., Fantle et al., 2010; Kastner, 1999; Paytan et al., 2021). A global estimation of the dissolving PIC fraction should account of this spatio-temporal variability and complex interactions of organic and inorganic particles within coastal sediments. Therefore, consideration of the detrital mineral flux of rivers to the ocean and its isotopic composition may help to solve longwithstanding debates about imbalances in global biogeochemical cycles.

# 5 Conclusion

The riverine flux of PIC, i.e., discharge of detrital carbonate minerals, represents a significant, yet mostly unaccounted chemical mass transfer in the Earth system (3.0 ± 0.4 Tmol C/y), currently contributing ~4 % to the total riverine carbon export. The pre-human flux was 4.0 ± 0.5 Tmol PIC/y; the 25 % reduction is caused by particle retention in reservoirs, especially of the Nile river. Considering perturbations of riverine particulate and dissolved, inorganic and organic carbon species in concert, the riverine export flux seems to have remained rather stable, while carbon speciation changed.

Although the fate of PIC in the ocean remains quantitatively unknown, oceanic element and isotope inventories of Ca and alkalinity are most probably affected by detrital carbonate dissolution in the coastal ocean, with implications for conclusions deduced from their highly debated, but frequently used mass balances. PIC contributions to the oceanic budgets of Sr and total C are less important and Mg fluxes are insignificant.

Naturally, the concentration of PIC is controlled by catchment topography and surface lithology, i.e., slowly changing tectonic factors ($10^3$ – $10^5$ y scales), but also by climate and vegetation, which are subjected to much faster spatio-temporal variations. Similarly, marine conditions change through time, so that related PIC dissolution may also vary. An additional, significant amount of detrital carbonate (0.7 ± 0.3 Tmol C/y) is exported from Greenland and Antarctica and responds to ice-sheet dynamics, while eolian contributions can be neglected (at the present). These results imply a response of the global PIC flux to human activity and to natural changes in environmental and climatic conditions, but also to the tectonic evolution of our planet.

## 6 Data and script accessibility

The all data and scripts used for this study, along with a detailed manual and the supplementary information, can can be accessed via: https://github.com/GerritMuller/Detrital-Carbonates-in-Earths-Element-cycles; INSERT ZENODO DOI HYPERLINK AFTER REVIEW.

## 7 Competing Interest

The authors declare that they have no conflict in interest.

## 8 Funding

This work was carried out under the program of the Netherlands Earth System Science Centre

(NESSC), financially supported by the Ministry of Education, Culture and Science (OCW). Funding was also provided by BMBF-project PALMOD (Ref 01LP1506C) through the German Federal Ministry of Education and Research (BMBF) as Research for Sustainability inititative (FONA). AS thanks the European Research Council for Consolidator Grant 771497.

## 9 Acknowledgements

We thank Olivier Sulpis, Jens Hartmann, Gibran Romero-Mujalli, Stefan Kempe and Jaap Nienhuis for discussion and advice.

## 10 References

Abril, G., Etcheber, H., Delille, B., Frankignoulle, M., & Borges, A. V. (2003). Carbonate dissolution in the turbid and eutrophic Loire estuary. *Marine Ecology Progress Series*, *259*, 129–138. https://doi.org/10.3354/meps259129

Aitkenhead, J. A., & McDowell, W. H. (2000). Soil C:N ratio as a predictor of annual riverine DOC flux at local and global scales. *Global Biogeochemical Cycles*, *14*(1), 127–138. https://doi.org/10.1029/1999GB900083

Aller, R. C. (1982). Carbonate dissolution in nearshore terrigenous muds: the role of physical and biological reworking. *Journal of Geology*, *90*(1), 79–95. https://doi.org/10.1086/628652

Aller, Robert C. (1994). Bioturbation and remineralization of sedimentary organic matter: effects of redox oscillation. *Chemical Geology*, *114*(3–4), 331–345. https://doi.org/10.1016/0009-2541(94)90062-0

Amiotte Suchet, P., Probst, J.-L., & Ludwig, W. (2003). Worldwide distribution of continental rock lithology: Implications for the atmospheric/soil CO 2 uptake by continental weathering and alkalinity river transport to the oceans . *Global Biogeochemical Cycles*, *17*(2), n/a-n/a. https://doi.org/10.1029/2002gb001891

Archer, D., Emerson, S., & Reimers, C. (1989). Dissolution of calcite in deep-sea sediments: pH and O2 microelectrode results. *Geochimica et Cosmochimica Acta*, *53*(11), 2831–2845. https://doi.org/10.1016/0016-7037(89)90161-0

Batjes, N. H. (2012). *ISRIC-WISE derived soil properties on a 5 by 5 arc-minutes global grid (ver. 1.2)*. ISRIC - World Soil Information.

Bayon, G., Toucanne, S., Skonieczny, C., André, L., Bermell, S., Cheron, S., et al. (2015). *Rare earth elements and neodymium isotopes in world river sediments revisited*. *Geochimica et Cosmochimica Acta* (Vol. 170). https://doi.org/10.1016/j.gca.2015.08.001

Beaulieu, E., Goddéris, Y., Labat, D., Roelandt, C., Calmels, D., & Gaillardet, J. (2011). Modeling of water-rock interaction in the Mackenzie basin: Competition between sulfuric and carbonic acids. *Chemical Geology*, *289*(1–2), 114–123. https://doi.org/10.1016/j.chemgeo.2011.07.020

Berner, E. K., & Berner, R. A. (2012). *Global environment : water, air, and geochemical cycles* (2nd ed.). Princeton, N.J.: Princeton University Press.

Berner, R A, Lasaga, A. C., & Garrels, R. M. (1983). The carbonate-silicate geochemical cycle ans its effect on atmospheric carbon dioxide over the past 100 million years. *American Journal of Science*, (283), 641–683.

Berner, Robert A. (1999). A New Look at the Long-term Carbon Cycle. *Gsa Today*, *9*(11), 1–6.

Berner, Robert A., & Berner, E. K. (1987). *Global environment: water, air, and geochemical cycles* (1st ed.). New Jersey: Prentice-Hall.

Berner, Robert A. (1982). Burial of organic carbon and pyrite sulfur in the modern ocean. *American Journal of Science*, *282*(4), 451–473.

Beusen, A. H. W., Dekkers, A. L. M., Bouwman, A. F., Ludwig, W., & Harrison, J. (2005). Estimation of global river transport of sediments and associated particulate C, N, and P. *Global Biogeochemical Cycles*, *19*(4). https://doi.org/10.1029/2005GB002453

Bond, G. C., & Lotti, R. (1995). Iceberg discharges into the North Atlantic on millennial time scales during the last glaciation. *Science*, *267*(5200), 1005–1010. https://doi.org/10.1126/science.267.5200.1005

Borges, A. V., & Gypens, N. (2010). Carbonate chemistry in the coastal zone responds more strongly to eutrophication than to ocean acidification. *Limnology and Oceanography*, *55*(1), 346–353. https://doi.org/10.4319/lo.2010.55.1.0346

Börker, J., Hartmann, J., Amann, T., & Romero-Mujalli, G. (2018). Terrestrial sediments of the earth: Development of a global unconsolidated sediments map database (gum). *Geochemistry, Geophysics, Geosystems*, *19*(4), 997–1024. https://doi.org/10.1002/2017GC007273

Bouchez, J., Gaillardet, J., France-Lanord, C., Maurice, L., & Dutra-Maia, P. (2011). Grain size control of river suspended sediment geochemistry: Clues from Amazon River depth profiles. *Geochemistry, Geophysics, Geosystems*, *12*(3), 1–24. https://doi.org/10.1029/2010GC003380

Boudreau, B. P., & Canfield, D. E. (1993). A comparison of closed- and open-system models for porewater pH and calcite-saturation state. *Geochimica et Cosmochimica Acta*, *57*(2), 317–334. https://doi.org/10.1016/0016-7037(93)90434-X

Boyer, E. W., & Howarth, R. W. (2008). Nitrogen Fluxes from Rivers to the Coastal Oceans. *Nitrogen in the Marine Environment*, (December), 1565–1587. https://doi.org/10.1016/B978-0-12-372522-6.00036-0

Brantley, S. L., White, A. F., & Kubicki, J. D. (2008). *Kinetics of water-rock interaction*. *Kinetics of Water-Rock Interaction*. https://doi.org/10.1007/978-0-387-73563-4

Brantley, S. L., Eissenstat, D. M., Marshall, J. A., Godsey, S. E., Balogh-Brunstad, Z., Karwan, D. L., et al. (2017). Reviews and syntheses: On the roles trees play in building and plumbing the critical zone. *Biogeosciences*, *14*(22), 5115–5142. https://doi.org/10.5194/bg-14-5115-2017

Broecker, W. S. (1982). Glacial to interglacial changes in ocean chemistry. *Progress in Oceanography*, *11*(2), 151–197. https://doi.org/10.1016/0079-6611(82)90007-6

Bufe, A., Hovius, N., Emberson, R., Rugenstein, J. K. C., Galy, A., Hassenruck-Gudipati, H. J., & Chang, J.-M. (2021). Co-variation of silicate, carbonate, and sulphide weathering drives CO2-release with erosion. *Nature Geoscience*, *14*(April), 211–216. https://doi.org/10.1038/s41561-021-00714-3

Burdige, D. J., Zimmerman, R. C., & Hu, X. (2008). Rates of carbonate dissolution in permeable sediments estimated from pore-water profiles: The role of sea grasses. *Limnology and Oceanography*, *53*(2), 549–565. https://doi.org/10.4319/lo.2008.53.2.0549

Cai, W. J., Hu, X., Huang, W. J., Murrell, M. C., Lehrter, J. C., Lohrenz, S. E., et al. (2011). Acidification of subsurface coastal waters enhanced by eutrophication. *Nature Geoscience*, *4*(11), 766–770. https://doi.org/10.1038/ngeo1297

Calmels, D., Gaillardet, J., Brenot, A., & France-Lanord, C. (2007). Sustained sulfide oxidation by physical erosion processes in the Mackenzie River basin: Climatic perspectives. *Geology*, *35*(11), 1003–1006. https://doi.org/10.1130/G24132A.1

Calmels, D., Gaillardet, J., & François, L. (2014). Sensitivity of carbonate weathering to soil CO2 production by biological activity along a temperate climate transect. *Chemical Geology*, *390*, 74–86. https://doi.org/10.1016/j.chemgeo.2014.10.010

Canfield, D. E. (1997). The geochemistry of river particulates from the continental USA: Major elements. *Geochimica et Cosmochimica Acta*, *61*(16), 3349–3365. https://doi.org/10.1016/S0016-7037(97)00172-5

Carstensen, J., & Duarte, C. M. (2019). Drivers of pH Variability in Coastal Ecosystems. *Environmental Science and Technology*, *53*(8), 4020–4029. https://doi.org/10.1021/acs.est.8b03655

Caves Rugenstein, J. K., Ibarra, D. E., & von Blanckenburg, F. (2019). Neogene cooling driven by land surface reactivity rather than increased weathering fluxes. *Nature*, *571*(7763), 99–102. https://doi.org/10.1038/s41586-019-1332-y

Chen, C., Guerit, L., Foreman, B. Z., Hassenruck-Gudipati, H. J., Adatte, T., Honegger, L., et al. (2018). Estimating regional flood discharge during Palaeocene-Eocene global warming. *Scientific Reports*, *8*(1), 1–8. https://doi.org/10.1038/s41598-018-31076-3

Chung, S.-N., Lee, K., Feely, R. A., Sabine, C. L., Millero, F. J., Wanninkhof, R., et al. (2003). Calcium carbonate budget in the Atlantic Ocean based on water column inorganic carbon chemistry. *Global Biogeochemical Cycles*, *17*(4), n/a-n/a. https://doi.org/10.1029/2002gb002001

Cohen, S., Kettner, A. J., & Syvitski, J. P. M. (2014). Global suspended sediment and water discharge dynamics between 1960 and 2010: Continental trends and intra-basin sensitivity. *Global and Planetary Change*, *115*, 44–58. https://doi.org/10.1016/j.gloplacha.2014.01.011

Cole, J. J., Prairie, Y. T., Caraco, N. F., McDowell, W. H., Tranvik, L. J., Striegl, R. G., et al. (2007). Plumbing the global carbon cycle: Integrating inland waters into the terrestrial carbon budget. *Ecosystems*, *10*(1), 171–184. https://doi.org/10.1007/s10021-006-9013-8

Conley, D. J. (2002). Terrestrial ecosystems and the global biogeochemical silica cycle. *Global Biogeochemical Cycles*, *16*(4), 68-1-68–8. https://doi.org/10.1029/2002gb001894

Dai, M., Yin, Z., Meng, F., Liu, Q., & Cai, W. J. (2012). Spatial distribution of riverine DOC inputs to the ocean: An updated global synthesis. *Current Opinion in Environmental Sustainability*, *4*(2), 170–178. https://doi.org/10.1016/j.cosust.2012.03.003

DePaolo, D. J. (2004). Calcium isotopic variations produced by biological, kinetic, radiogenic and nucleosynthetic processes. *Reviews in Mineralogy and Geochemistry*, *55*, 255–288. https://doi.org/10.2138/gsrmg.55.1.255

Dickens, G. R. (2001). Carbon addition and removal during the late Palaeocene thermal maximum: Basic theory with a preliminary treatment of the isotopic record at ODP Site 1051, Blake Nose. *Geological Society Special Publication*, *183*(May 2007), 293–305.

https://doi.org/10.1144/GSL.SP.2001.183.01.14

Dixon, J. L., & von Blanckenburg, F. (2012). Soils as pacemakers and limiters of global silicate weathering. *Comptes Rendus - Geoscience*, *344*(11–12), 597–609. https://doi.org/10.1016/j.crte.2012.10.012

Dixon, J. L., Chadwick, O. A., & Vitousek, P. M. (2016). Climate-driven thresholds for chemical weathering in postglacial soils of New Zealand Jean. *Journal of Geophysical Research: Earth Surface RESEARCH*, 1619–1634. https://doi.org/doi:10.1002/2016JF003864

Dornblaser, M. M., & Striegl, R. G. (2009). Suspended sediment and carbonate transport in the Yukon River Basin, Alaska: Fluxes and potential future responses to climate change. *Water Resources Research*, *45*(6). https://doi.org/10.1029/2008WR007546

Drake, T. W., Tank, S. E., Zhulidov, A. V., Holmes, R. M., Gurtovaya, T., & Spencer, R. G. M. (2018). Increasing Alkalinity Export from Large Russian Arctic Rivers. *Environmental Science and Technology*, *52*(15), 8302–8308. https://doi.org/10.1021/acs.est.8b01051

Dyer, K. R. (1995). Sediment transport processes in estuaries. *Developments in Sedimentology*, *53*(C), 423–449. https://doi.org/10.1016/S0070-4571(05)80034-2

Ebelmen, J.-J. (1845). Sur les produits de la décomposition des espèces minérales de la famille des silicates. In *Annales des Mines* (Vol. 7, p. 66).

Fantle, M. S., Maher, K. M., & Depaolo, D. J. (2010). Isotopic approaches for quantifying the rates of marine burial diagenesis. *Reviews of Geophysics*, *48*(3), 1–38. https://doi.org/10.1029/2009RG000306

Ferrier, K. L., & West, N. (2017). Responses of chemical erosion rates to transient perturbations in physical erosion rates, and implications for relationships between chemical and physical erosion rates in regolith-mantled hillslopes. *Earth and Planetary Science Letters*, *474*, 447–456. https://doi.org/10.1016/j.epsl.2017.07.002

Filippelli, G. M., Latimer, J. C., Murray, R. W., & Flores, J. A. (2007). Productivity records from the Southern Ocean and the equatorial Pacific Ocean: Testing the glacial Shelf-Nutrient Hypothesis. *Deep-Sea Research Part II: Topical Studies in Oceanography*, *54*(21–22), 2443–2452. https://doi.org/10.1016/j.dsr2.2007.07.021

Fletcher, D., MacKenzie, D., & Villouta, E. (2005). Modelling skewed data with many zeros: A simple approach combining ordinary and logistic regression. *Environmental and Ecological Statistics*, *12*(1), 45–54. https://doi.org/10.1007/s10651-005-6817-1

Foreman, B. Z., Heller, P. L., & Clementz, M. T. (2012). Fluvial response to abrupt global warming at the Palaeocene/Eocene boundary. *Nature*, *491*(7422), 92–95. https://doi.org/10.1038/nature11513

Foster, G. L., & Vance, D. (2006). Negligible glacial-interglacial variation in continental chemical weathering rates. *Nature*, *444*(7121), 918–921. https://doi.org/10.1038/nature05365

France-Lanord, C., Galy, A., & Rigaudier, T. (2018). Detrital, biogenic, and diagenetic carbonates in turbidites of the Bengal Fan. In *Goldschmidt Conference 2018*. Boston, United States. Retrieved from https://hal.archives-ouvertes.fr/hal-02328548

Friedlingstein, P., O'Sullivan, M., Jones, M. W., Andrew, R. M., Hauck, J., Olsen, A., et al. (2020). Global Carbon Budget 2020. *Earth System Science Data*, *12*(4), 3269–3340. https://doi.org/10.5194/essd-12-3269-2020

Froelich, P. N., Bender, M. L., Luedtke, N. A., Heath, G. R., & DeVries, T. (1982). The marine

phosphorous cycle. *American Journa of Science*, *282*, 474–511.

Gaillardet, J., Dupré, B., & Allègre, C. J. (1999). Geochemistry of large river suspended sediments: Silicate weathering or recycling tracer? *Geochimica et Cosmochimica Acta*, *63*(23–24), 4037–4051. https://doi.org/10.1016/s0016-7037(99)00307-5

Gaillardet, Jérôme, Calmels, D., Romero-Mujalli, G., Zakharova, E., & Hartmann, J. (2019). Global climate control on carbonate weathering intensity. *Chemical Geology*, *527*(May), 1–11. https://doi.org/10.1016/j.chemgeo.2018.05.009

Galy, V., Peucker-Ehrenbrink, B., & Eglinton, T. (2015). Global carbon export from the terrestrial biosphere controlled by erosion. *Nature*, *521*(7551), 204–207. https://doi.org/10.1038/nature14400

Gandomi, A. H., Alavi, A. H., & Ryan, C. (2015). *Handbook of genetic programming applications*. *Handbook of Genetic Programming Applications*. https://doi.org/10.1007/978-3-319-20883-1

Ganeshram, S., Pedersen, F., Calvert, E., Mcneill, W., & Fontugne, M. R. (2000). in the world ' s oceans : Causes and consequences. *Paleoceanography*, *15*(4), 361–376.

Garzanti, E., Andó, S., France-Lanord, C., Censi, P., Vignola, P., Galy, V., & Lupker, M. (2011). Mineralogical and chemical variability of fluvial sediments 2. Suspended-load silt (Ganga-Brahmaputra, Bangladesh). *Earth and Planetary Science Letters*, *302*(1–2), 107–120. https://doi.org/10.1016/j.epsl.2010.11.043

Gattuso, J. P., Frankignoulle, M., & Wollast, R. (1998). Carbon and Carbonate Metabolism in Coastal Aquatic Ecosystems Author ( s ): J . -P . Gattuso , M . Frankignoulle and R . Wollast Source : Annual Review of Ecology and Systematics , Vol . 29 ( 1998 ), pp . 405-434 Published by : Annual Reviews Stable URL : *Annual Reviews in Ecology and Systematics*, *29*(1998), 405–434.

Gislason, S. R., Oelkers, E. H., & Snorrason, Á. (2006). Role of river-suspended material in the global carbon cycle. *Geology*, *34*(1), 49–52. https://doi.org/10.1130/G22045.1

Govers, G., Van Oost, K., & Wang, Z. (2014). Scratching the Critical Zone: The Global Footprint of Agricultural Soil Erosion. *Procedia Earth and Planetary Science*, *10*, 313–318. https://doi.org/10.1016/j.proeps.2014.08.023

Grosbois, C., Négrel, P., Grimaud, D., & Fouillac, C. (2001). An overview of dissolved and suspended matter fluxes in the Loire River Basin: Natural and anthropogenic inputs. *Aquatic Geochemistry*, *7*(2), 81–105. https://doi.org/10.1023/A:1017518831860

Gu, D., Zhang, L., & Jiang, L. (2009). The effects of estuarine processes on the fluxes of inorganic and organic carbon in the Yellow River estuary. *Journal of Ocean University of China*, *8*(4), 352–358. https://doi.org/10.1007/s11802-009-0352-x

Harrison, J. A., Caraco, N., & Seitzinger, S. P. (2005). Global patterns and sources of dissolved organic matter export to the coastal zone: Results from a spatially explicit, global model. *Global Biogeochemical Cycles*, *19*(4). https://doi.org/10.1029/2005GB002480

Hartmann, J., & Moosdorf, N. (2012). The new global lithological map database GLiM: A representation of rock properties at the Earth surface. *Geochemistry, Geophysics, Geosystems*, *13*(12), 1–37. https://doi.org/10.1029/2012GC004370

Hartmann, J., Moosdorf, N., Lauerwald, R., Hinderer, M., & West, A. J. (2014). Global chemical weathering and associated p-release - the role of lithology, temperature and soil properties. *Chemical Geology*, *363*, 145–163. https://doi.org/10.1016/j.chemgeo.2013.10.025

Haynes, R. J., & Naidu, R. (1998). Influence of lime, fertilizer and manure applications on soil organic

matter. *Nutrient Cycling in Agroecosystems*, *51*(123), 123–137. Retrieved from http://link.springer.com/article/10.1023/A:1009738307837

Hilton, R. G., & West, A. J. (2020). Mountains, erosion and the carbon cycle. *Nature Reviews Earth & Environment*, *1*(6), 284–299. https://doi.org/10.1038/s43017-020-0058-6

Hong, W. L., Torres, M. E., & Kutterolf, S. (2020). Towards a global quantification of volcanogenic aluminosilicate alteration rates through the mass balance of strontium in marine sediments. *Chemical Geology*, *550*(October 2019), 119743. https://doi.org/10.1016/j.chemgeo.2020.119743

Horvath, A. (2004). Construction materials and the environment. *Annual Review of Environment and Resources*, *29*, 181–204. https://doi.org/10.1146/annurev.energy.29.062403.102215

Huang, Q. bo, Qin, X. qun, Liu, P. yu, Zhang, L. kai, & Su, C. tian. (2017). Impact of sulfuric and nitric acids on carbonate dissolution, and the associated deficit of CO2 uptake in the upper–middle reaches of the Wujiang River, China. *Journal of Contaminant Hydrology*, *203*(December 2016), 18–27. https://doi.org/10.1016/j.jconhyd.2017.05.006

Jenny, H. (1941). *Factors of soil formation: A System of Pedology*. *Soils: Basic Concepts and Future Challenges* (Vol. 9780521851). New York: McGraw-Hill book Company. https://doi.org/10.1017/CBO9780511535802.014

Jickells, T. D., An, Z. S., Andersen, K. K., Baker, A. R., Bergametti, C., Brooks, N., et al. (2005). Global iron connections between desert dust, ocean biogeochemistry, and climate. *Science*, *308*(5718), 67–71. https://doi.org/10.1126/science.1105959

Jin, Y., Fu, W., Kang, J., Guo, J., & Guo, J. (2019). Bayesian symbolic regression. *ArXiv*.

Jones, M. T., Pearce, C. R., Jeandel, C., Gislason, S. R., Eiriksdottir, E. S., Mavromatis, V., & Oelkers, E. H. (2012). Riverine particulate material dissolution as a significant flux of strontium to the oceans. *Earth and Planetary Science Letters*, *355–356*, 51–59. https://doi.org/10.1016/j.epsl.2012.08.040

Journet, E., Balkanski, Y., & Harrison, S. P. (2014). A new data set of soil mineralogy for dust-cycle modeling. *Atmospheric Chemistry and Physics*, *14*(8), 3801–3816. https://doi.org/10.5194/acp-14-3801-2014

Kastner, M. (1999). Oceanic minerals: Their origin, nature of their environment, and significance. *Proceedings of the National Academy of Sciences of the United States of America*, *96*(7), 3380–3387. https://doi.org/10.1073/pnas.96.7.3380

Kempe, S., & Emeis, K. (1985). Carboante Chemistry and the Formation of Plitvice Lake. *Mitt. Geol.-Paläont. Inst. Univ. Hamburg*, *SCOPE/UNEP*, 351–383.

Kitsikoudis, V., Sidiropoulos, E., & Hrissanthou, V. (2013). Derivation of Sediment Transport Models for Sand Bed Rivers from Data-Driven Techniques. *Sediment Transport Processes and Their Modelling Applications*, (September 2015). https://doi.org/10.5772/53432

Koehler, E., Brown, E., & Haneuse, S. J.-P. A. (2009). On the Assessment of Monte Carlo Error in Simulation-Based Statistical Analyses. *Am. Stat.*, *63*(2), 1-155–162. https://doi.org/10.1198/tast.2009.0030.On

Krabbenhöft, A., Eisenhauer, A., Böhm, F., Vollstaedt, H., Fietzke, J., Liebetrau, V., et al. (2010). Constraining the marine strontium budget with natural strontium isotope fractionations (87Sr/86Sr*, δ88/86Sr) of carbonates, hydrothermal solutions and river waters. *Geochimica et Cosmochimica Acta*, *74*(14), 4097–4109. https://doi.org/10.1016/j.gca.2010.04.009

739 Krumins, V., Gehlen, M., Arndt, S., Van Cappellen, P., & Regnier, P. (2013). Dissolved inorganic
740 carbon and alkalinity fluxes from coastal marine sediments: Model estimates for different shelf
741 environments and sensitivity to global change. *Biogeosciences*, *10*(1), 371–398.
742 https://doi.org/10.5194/bg-10-371-2013

743 Kump, L. R., & Alley, R. B. (1994). Global chemical weathering on glacial time scales. *Material Fluxes*
744 *on the Surface of the Earth*, 46–60.

745 Kuylen, A. A. A., & Verhallen, T. M. M. (1981). The use of canonical analysis. *Journal of Economic*
746 *Psychology*, *1*(3), 217–237. https://doi.org/10.1016/0167-4870(81)90039-8

747 Lambert, T., Bouillon, S., Darchambeau, F., Morana, C., Roland, F. A. E., Descy, J. P., & Borges, A. V.
748 (2017). Effects of human land use on the terrestrial and aquatic sources of fluvial organic
749 matter in a temperate river basin (The Meuse River, Belgium). *Biogeochemistry*, *136*(2), 191–
750 211. https://doi.org/10.1007/s10533-017-0387-9

751 Lasaga, A. C. (1984). Chemical Kinetics of Water-Rock Interactions. *Journal of Geophysical Research*,
752 *89*(4), 4009–4025.

753 Lebrato, M., Garbe-Schönberg, D., Müller, M. N., Blanco-Ameijeiras, S., Feely, R. A., Lorenzoni, L., et
754 al. (2020). Global variability in seawater Mg:Ca and Sr:Ca ratios in the modern ocean.
755 *Proceedings of the National Academy of Sciences of the United States of America*, *117*(36),
756 22281–22292. https://doi.org/10.1073/pnas.1918943117

757 Li, M., Peng, C., Wang, M., Xue, W., Zhang, K., Wang, K., et al. (2017). The carbon flux of global rivers:
758 A re-evaluation of amount and spatial patterns. *Ecological Indicators*, *80*(April), 40–51.
759 https://doi.org/10.1016/j.ecolind.2017.04.049

760 Li, M., Peng, C., Zhou, X., Yang, Y., Guo, Y., Shi, G., & Zhu, Q. (2019). Modeling Global Riverine DOC
761 Flux Dynamics From 1951 to 2015. *Journal of Advances in Modeling Earth Systems*, *11*(2), 514–
762 530. https://doi.org/10.1029/2018MS001363

763 Linke, S., Lehner, B., Ouellet Dallaire, C., Ariwi, J., Grill, G., Anand, M., et al. (2019). Global hydro-
764 environmental sub-basin and river reach characteristics at high spatial resolution. *Scientific*
765 *Data*, *6*(1), 283. https://doi.org/10.1038/s41597-019-0300-6

766 Liu, D., Bai, Y., He, X., Chen, C. T. A., Huang, T. H., Pan, D., et al. (2020). Changes in riverine organic
767 carbon input to the ocean from mainland China over the past 60 years. *Environment*
768 *International*, *134*(May 2019), 105258. https://doi.org/10.1016/j.envint.2019.105258

769 Liu, Z., Macpherson, G. L., Groves, C., Martin, J. B., Yuan, D., & Zeng, S. (2018). Large and active CO2
770 uptake by coupled carbonate weathering. *Earth-Science Reviews*, *182*(December 2017), 42–49.
771 https://doi.org/10.1016/j.earscirev.2018.05.007

772 Ludwig, W., Amiotte-Suchet, P., & Probst, J. L. (1996). River discharges of carbon to the world's
773 oceans: Determining local inputs of alkalinity and of dissolved and particulate organic carbon.
774 *Comptes Rendus de l'Academie de Sciences - Serie IIa: Sciences de La Terre et Des Planetes*,
775 *323*(12), 1007–1014.

776 Ludwig, W., Amiotte-Suchet, P., Munhoven, G., & Probst, J. L. (1998). Atmospheric CO2 consumption
777 by continental erosion: Present-day controls and implications for the last glacial maximum.
778 *Global and Planetary Change*, *16–17*, 107–120. https://doi.org/10.1016/S0921-8181(98)00016-
779 2

780 Luo, M., Torres, M. E., Hong, W. L., Pape, T., Fronzek, J., Kutterolf, S., et al. (2020). Impact of iron
781 release by volcanic ash alteration on carbon cycling in sediments of the northern Hikurangi
782 margin. *Earth and Planetary Science Letters*, *541*, 116288.

https://doi.org/10.1016/j.epsl.2020.116288

Ma, L., Jin, L., & Brantley, S. L. (2011). Geochemical behaviors of different element groups during shale weathering at the Susquehanna/Shale Hills Critical Zone Observatory. *Applied Geochemistry*, *26*(SUPPL.), S89–S93. https://doi.org/10.1016/j.apgeochem.2011.03.038

Maavara, T., Lauerwald, R., Regnier, P., & Van Cappellen, P. (2017). Global perturbation of organic carbon cycling by river damming. *Nature Communications*, *8*(May), 1–10. https://doi.org/10.1038/ncomms15347

Mackenzie, F. T., & Garrels, R. M. (1966). Chemical mass balance between rivers and oceans. *American Journal of Science*, *264*(7), 507–525. https://doi.org/10.2475/ajs.264.7.507

Mackenzie, Fred T., & Andersson, A. J. (2011). Biological control on diagenesis: Influence of bacteria and relevance to ocean acidification. *Encyclopedia of Earth Sciences Series*, (9781402092114), 137–143. https://doi.org/10.1007/978-1-4020-9212-1_73

Mackenzie, Fred T, & Garrels, R. M. (1965). Silicates : Reactivity with Sea Water Published by : American Association for the Advancement of Science Stable URL : https://www.jstor.org/stable/1717960, *150*(3692), 57–58.

Mayfield, K. K., Eisenhauer, A., Santiago Ramos, D. P., Higgins, J. A., Horner, T. J., Auro, M., et al. (2021). Groundwater discharge impacts marine isotope budgets of Li, Mg, Ca, Sr, and Ba. *Nature Communications*, *12*(1), 1–9. https://doi.org/10.1038/s41467-020-20248-3

Meade, R. H. (1972). Transport and Deposition of Sediments in Estuaries. In B. W. Nelson (Ed.), *Environmental Framework of Coastal Plain Estuaries* (Vol. 133, p. 0). Geological Society of America. https://doi.org/10.1130/MEM133-p91

Meybeck, M. (1982). Carbon, nitrogen, and phosphorus transport by world rivers. *American Journal of Science*. https://doi.org/10.2475/ajs.282.4.401

Meybeck, M. (1993). C, N, P and S in Rivers: From Sources to Global Inputs BT - Interactions of C, N, P and S Biogeochemical Cycles and Global Change, *I*(i), 163–193. Retrieved from https://doi.org/10.1007/978-3-642-76064-8_6

Middelburg, J. J., Soetaert, K., & Hagens, M. (2020). Ocean Alkalinity, Buffering and Biogeochemical Processes. *Reviews of Geophysics*, *58*(3). https://doi.org/10.1029/2019RG000681

Milliman, J. D., & Syvitski, J. P. M. (1992). Geomorphic/tectonic control of sediment discharge to the ocean: the importance of small mountainous rivers. *Journal of Geology*, *100*(5), 525–544. https://doi.org/10.1086/629606

Milliman, John D. (1974). *Marine carbonates*. *Springer*. https://doi.org/10.1177/1464884910394285

Milliman, John D., & Farnsworth, K. L. (2011). *River discharge to the coastal ocean: A global synthesis*. *River Discharge to the Coastal Ocean: A Global Synthesis*. https://doi.org/10.1017/CBO9780511781247

Milliman, John D. (1993). Production and accumulation of calcium carbonate in the ocean: Budget of a nonsteady state. *Global Biogeochemical Cycles*, *7*(4), 927–957.

Morse, J. W., & Arvidson, R. S. (2002). The dissolution kinetics of major sedimentary carbonate minerals. *Earth-Science Reviews*, *58*(1–2), 51–84. https://doi.org/10.1016/S0012-8252(01)00083-6

Mouyen, M., Longuevergne, L., Steer, P., Crave, A., Lemoine, J. M., Save, H., & Robin, C. (2018). Assessing modern river sediment discharge to the ocean using satellite gravimetry. *Nature*

*Communications*, *9*(1), 1–9. https://doi.org/10.1038/s41467-018-05921-y

Müller, G., Middelburg, J. J., & Sluijs, A. (2021a). Global River Sediments (GloRiSe). Zenodo. https://doi.org/10.5281/zenodo.4447435

Müller, G., Middelburg, J. J., & Sluijs, A. (2021b). Introducing GloRiSe - A global database on river sediment composition. *Earth System Science Data*, *13*, 3565–3575. https://doi.org/https://doi.org/10.5194/essd-13-3565-202

Négrel, P., & Grosbois, C. (1999). Changes in chemical and 87Sr/86Sr signature distribution patterns of suspended matter and bed sediments in the upper Loire river basin (France). *Chemical Geology*, *156*(1–4), 231–249. https://doi.org/10.1016/S0009-2541(98)00182-X

Nesbitt, W. A., & Mucci, A. (2021). Direct evidence of sediment carbonate dissolution in response to bottom-water acidification in the gulf of st. Lawrence, canada. *Canadian Journal of Earth Sciences*, *58*(1), 84–92. https://doi.org/10.1139/cjes-2020-0020

Nienhuis, J. H., Ashton, A. D., Edmonds, D. A., Hoitink, A. J. F., Kettner, A. J., Rowland, J. C., & Törnqvist, T. E. (2020). Global-scale human impact on delta morphology has led to net land area gain. *Nature*, *577*(7791), 514–518. https://doi.org/10.1038/s41586-019-1905-9

Noacco, V., Wagener, T., Worrall, F., Burt, T. P., & Howden, N. J. K. (2017). Human impact on long-term organic carbon export to rivers. *Journal of Geophysical Research: Biogeosciences*, *122*(4), 947–965. https://doi.org/10.1002/2016JG003614

O'Mara, N. A., & Dunne, J. P. (2019). Hot Spots of Carbon and Alkalinity Cycling in the Coastal Oceans. *Scientific Reports*, *9*(1), 1–8. https://doi.org/10.1038/s41598-019-41064-w

Oelkers, E. H., Golubev, S. V., Pokrovsky, O. S., & Bénézeth, P. (2011). Do organic ligands affect calcite dissolution rates? *Geochimica et Cosmochimica Acta*, *75*(7), 1799–1813. https://doi.org/10.1016/j.gca.2011.01.002

Overeem, I., Hudson, B. D., Syvitski, J. P. M., Mikkelsen, A. B., Hasholt, B., Van Den Broeke, M. R., et al. (2017). Substantial export of suspended sediment to the global oceans from glacial erosion in Greenland. *Nature Geoscience*, *10*(11), 859–863. https://doi.org/10.1038/NGEO3046

Pasquier, V., Revillon, S., Leroux, E., Molliex, S., Mocochain, L., & Rabineau, M. (2019). Quantifying biogenic versus detrital carbonates on marine shelf: An isotopic approach. *Frontiers in Earth Science*, *7*(July), 1–10. https://doi.org/10.3389/feart.2019.00164

Paytan, A., Griffith, E. M., Eisenhauer, A., Hain, M. P., Wallmann, K., & Ridgwell, A. (2021). A 35-million-year record of seawater stable Sr isotopes reveals a fluctuating global carbon cycle. *Science*, *371*(6536), 1346–1350. https://doi.org/10.1126/science.aaz9266

Penman, D. E., Caves Rugenstein, J. K., Ibarra, D. E., & Winnick, M. J. (2020). Silicate weathering as a feedback and forcing in Earth's climate and carbon cycle. *Earth-Science Reviews*, *209*, 103298. https://doi.org/10.1016/j.earscirev.2020.103298

Perrin, A. S., Probst, A., & Probst, J. L. (2008). Impact of nitrogenous fertilizers on carbonate dissolution in small agricultural catchments: Implications for weathering CO2 uptake at regional and global scales. *Geochimica et Cosmochimica Acta*, *72*(13), 3105–3123. https://doi.org/10.1016/j.gca.2008.04.011

Peterson, M. N. A. (1966). Calcite: Rates of dissolution in a vertical profile in the central pacific. *Science*, *154*(3756), 1542–1544. https://doi.org/10.1126/science.154.3756.1542

van der Ploeg, R., Boudreau, B. P., Middelburg, J. J., & Sluijs, A. (2019). Cenozoic carbonate burial along continental margins. *Geology*, *47*(11), 1025–1028. https://doi.org/10.1130/G46418.1

Pokrovsky, O. S., Golubev, S. V., & Schott, J. (2005). Dissolution kinetics of calcite, dolomite and magnesite at 25 °C and 0 to 50 atm pCO2. *Chemical Geology*, *217*(3-4 SPEC. ISS.), 239–255. https://doi.org/10.1016/j.chemgeo.2004.12.012

Poulton, S. W., & Raiswell, R. (2002). The low-temperature geochemical cycle of iron: From continental fluxes to marine sediment deposition. *American Journal of Science*, *302*(9), 774–805. https://doi.org/10.2475/ajs.302.9.774

Raiswell, R., Benning, L. G., Tranter, M., & Tulaczyk, S. (2008). Bioavailable iron in the Southern Ocean: The significance of the iceberg conveyor belt. *Geochemical Transactions*, *9*, 1–9. https://doi.org/10.1186/1467-4866-9-7

Raymond, P. A., & Hamilton, S. K. (2018). Anthropogenic influences on riverine fluxes of dissolved inorganic carbon to the oceans. *Limnology and Oceanography Letters*, *3*(3), 143–155. https://doi.org/10.1002/lol2.10069

Regnier, P., Friedlingstein, P., Ciais, P., Mackenzie, F. T., Gruber, N., Janssens, I. A., et al. (2013). Anthropogenic perturbation of the carbon fluxes from land to ocean. *Nature Geoscience*, *6*(8), 597–607. https://doi.org/10.1038/ngeo1830

Resplandy, L., Keeling, R. F., Rödenbeck, C., Stephens, B. B., Khatiwala, S., Rodgers, K. B., et al. (2018). Revision of global carbon fluxes based on a reassessment of oceanic and riverine carbon transport. *Nature Geoscience*, *11*(7), 504–509. https://doi.org/10.1038/s41561-018-0151-3

Rueda, F., Moreno-Ostos, E., & Armengol, J. (2006). The residence time of river water in reservoirs. *Ecological Modelling*, *191*(2), 260–274. https://doi.org/10.1016/j.ecolmodel.2005.04.030

Saderne, V., Geraldi, N. R., Macreadie, P. I., Maher, D. T., Middelburg, J. J., Serrano, O., et al. (2019). Role of carbonate burial in Blue Carbon budgets. *Nature Communications*, *10*(1). https://doi.org/10.1038/s41467-019-08842-6

Santos, I. R., Maher, D. T., Larkin, R., Webb, J. R., & Sanders, C. J. (2019). Carbon outwelling and outgassing vs. burial in an estuarine tidal creek surrounded by mangrove and saltmarsh wetlands. *Limnology and Oceanography*, *64*(3), 996–1013. https://doi.org/10.1002/lno.11090

Savenko, V. S. (2007). Chemical composition of sediment load carried by rivers. *Geochemistry International*, *45*(8), 816–824. https://doi.org/10.1134/S0016702907080071

Schachtman, N. S., Roering, J. J., Marshall, J. A., Gavin, D. G., & Granger, D. E. (2019). The interplay between physical and chemical erosion over glacial-interglacial cycles. *Geology*, *47*(7), 613–616. https://doi.org/10.1130/G45940.1

van de Schootbrugge, B., van der Weijst, C. M. H., Hollaar, T. P., Vecoli, M., Strother, P. K., Kuhlmann, N., et al. (2020). Catastrophic soil loss associated with end-Triassic deforestation. *Earth-Science Reviews*, *210*(August), 103332. https://doi.org/10.1016/j.earscirev.2020.103332

Schrag, D. P. (2013). Authigenic carbonate and the history of the global carbon cycle. *Science*, *339*(6126), 540–543. https://doi.org/10.1126/science.339.6126.1383-b

Searson, D. P., Leahy, D. E., & Willis, M. J. (2010). GPTIPS:An open source genetic programming toolbox for multigene symbolic regression. *Proceedings of the International MultiConference of Engineers and Computer Scientists 2010, IMECS 2010*, *I*, 77–80.

Shalev, N., Bontognali, T. R. R., Wheat, C. G., & Vance, D. (2019). New isotope constraints on the Mg oceanic budget point to cryptic modern dolomite formation. *Nature Communications*, *10*(1), 1–10. https://doi.org/10.1038/s41467-019-13514-6

911 Shen, C., Testa, J. M., Li, M., Cai, W. J., Waldbusser, G. G., Ni, W., et al. (2019). Controls on Carbonate
912 System Dynamics in a Coastal Plain Estuary: A Modeling Study. *Journal of Geophysical Research:*
913 *Biogeosciences*, *124*(1), 61–78. https://doi.org/10.1029/2018JG004802

914 Shoghi Kalkhoran, S., Pannell, D. J., Thamo, T., White, B., & Polyakov, M. (2019). Soil acidity, lime
915 application, nitrogen fertility, and greenhouse gas emissions: Optimizing their joint economic
916 management. *Agricultural Systems*, *176*(September), 102684.
917 https://doi.org/10.1016/j.agsy.2019.102684

918 Sluijs, A., Zeebe, R. E., Bijl, P. K., & Bohaty, S. M. (2013). A middle Eocene carbon cycle conundrum.
919 *Nature Geoscience*, *6*(6), 429–434. https://doi.org/10.1038/ngeo1807

920 Sulpis, O., Lix, C., Mucci, A., & Boudreau, B. P. (2017). Calcite dissolution kinetics at the sediment-
921 water interface in natural seawater. *Marine Chemistry*, *195*(September 2018), 70–83.
922 https://doi.org/10.1016/j.marchem.2017.06.005

923 Sutton, J. N., André, L., Cardinal, D., Conley, D. J., Souza, G. F. De, Dean, J., et al. (2018). A Review of
924 the Stable Isotope Bio-geochemistry of the Global Silicon Cycle and Its Associated Trace
925 Elements, *5*(January). https://doi.org/10.3389/feart.2017.00112

926 Syvitski, J. P. M., & Kettner, A. (2011). Sediment flux and the anthropocene. *Philosophical*
927 *Transactions of the Royal Society A: Mathematical, Physical and Engineering Sciences*,
928 *369*(1938), 957–975. https://doi.org/10.1098/rsta.2010.0329

929 Syvitski, J. P. M., Vörösmarty, C. J., Kettner, A. J., & Green, P. (2005). Impact of Humans on the Flux
930 of Terrestrial Sediment to the Global Coastal Ocean. *Science*, *308*(April), 376–381.
931 https://doi.org/10.1126/science.1109454

932 Tipper, E. T., Galy, A., Gaillardet, J., Bickle, M. J., Elderfield, H., & Carder, E. A. (2006). The magnesium
933 isotope budget of the modern ocean: Constraints from riverine magnesium isotope ratios.
934 *Earth and Planetary Science Letters*, *250*(1–2), 241–253.
935 https://doi.org/10.1016/j.epsl.2006.07.037

936 Tipper, E. T., Gaillardet, J., Galy, A., Louvat, P., Bickle, M. J., & Capmas, F. (2010). Calcium isotope
937 ratios in the world's largest rivers: A constraint on the maximum imbalance of oceanic calcium
938 fluxes. *Global Biogeochemical Cycles*, *24*(3). https://doi.org/10.1029/2009GB003574

939 Tipper, Edward T., Stevenson, E. I., Alcock, V., Knight, A. C. G., Baronas, J. J., Hilton, R. G., et al.
940 (2021). Global silicate weathering flux overestimated because of sediment-water cation
941 exchange. *Proceedings of the National Academy of Sciences of the United States of America*,
942 *118*(1). https://doi.org/10.1073/pnas.2016430118

943 Torres, M. A., West, A. J., & Li, G. (2014). Sulphide oxidation and carbonate dissolution as a source of
944 CO2 over geological timescales. *Nature*, *507*(7492), 346–349.
945 https://doi.org/10.1038/nature13030

946 Torres, M. A., Moosdorf, N., Hartmann, J., Adkins, J. F., & West, A. J. (2017). Glacial weathering,
947 sulfide oxidation, and global carbon cycle feedbacks. *Proceedings of the National Academy of*
948 *Sciences of the United States of America*, *114*(33), 8716–8721.
949 https://doi.org/10.1073/pnas.1702953114

950 Torres, M. E., Hong, W. L., Solomon, E. A., Milliken, K., Kim, J. H., Sample, J. C., et al. (2020). Silicate
951 weathering in anoxic marine sediment as a requirement for authigenic carbonate burial. *Earth-*
952 *Science Reviews*, *200*(September 2019), 102960.
953 https://doi.org/10.1016/j.earscirev.2019.102960

954 Tsandev, I., Rabouille, C., Slomp, C. P., & Van Cappellen, P. (2010). Shelf erosion and submarine river

canyons: Implications for deep-sea oxygenation and ocean productivity during glaciation. *Biogeosciences*, *7*(6), 1973–1982. https://doi.org/10.5194/bg-7-1973-2010

Urey, H. (1952). On the early chemical history of the earth and the origin of life. *Geophysics*, *38*, 351–363.

Viers, J., Dupré, B., & Gaillardet, J. (2009). Chemical composition of suspended sediments in World Rivers: New insights from a new database. *Science of the Total Environment*, *407*(2), 853–868. https://doi.org/10.1016/j.scitotenv.2008.09.053

Wadham, J. L., De'Ath, R., Monteiro, F. M., Tranter, M., Ridgwell, A., Raiswell, R., & Tulaczyk, S. (2013). The potential role of the Antarctic Ice Sheet in global biogeochemical cycles. *Earth and Environmental Science Transactions of the Royal Society of Edinburgh*, *104*(1), 55–67. https://doi.org/10.1017/S1755691013000108

Wallace, R. B., Baumann, H., Grear, J. S., Aller, R. C., & Gobler, C. J. (2014). Coastal ocean acidification: The other eutrophication problem. *Estuarine, Coastal and Shelf Science*, *148*, 1–13. https://doi.org/10.1016/j.ecss.2014.05.027

Walz, J., Knoblauch, C., Böhme, L., & Pfeiffer, E. M. (2017). Regulation of soil organic matter decomposition in permafrost-affected Siberian tundra soils - Impact of oxygen availability, freezing and thawing, temperature, and labile organic matter. *Soil Biology and Biochemistry*, *110*, 34–43. https://doi.org/10.1016/j.soilbio.2017.03.001

Webb, J. A., & Sasowsky, I. D. (1994). The interaction of acid mine drainage with a carbonate terrane: evidence from the Obey River, north-central Tennessee. *Journal of Hydrology*, *161*(327–346).

West, A. J., Galy, A., & Bickle, M. (2005). Tectonic and climatic controls on silicate weathering. *Earth and Planetary Science Letters*, *235*(1–2), 211–228. https://doi.org/10.1016/j.epsl.2005.03.020

West, J. A. (2012). Thickness of the chemical weathering zone and implications for erosional and climatic drivers of weathering and for carbon-cycle feedbacks. *Geology*, *40*(9), 811–814. https://doi.org/10.1130/G33041.1

White, L. F., Bailey, I., Foster, G. L., Allen, G., Kelley, S. P., Andrews, J. T., et al. (2016). Tracking the provenance of Greenland-sourced, Holocene aged, individual sand-sized ice-rafted debris using the Pb-isotope compositions of feldspars and 40Ar/39Ar ages of hornblendes. *Earth and Planetary Science Letters*, *433*(January), 192–203. https://doi.org/10.1016/j.epsl.2015.10.054

Wicks, C. M., & Groves, C. G. (1993). Acidic mine drainage in carbonate terrains: geochemical processes and rates of calcite dissolution. *Journal of Hydrology*, *146*(C), 13–27. https://doi.org/10.1016/0022-1694(93)90267-D

Willenbring, J. K., & Von Blanckenburg, F. (2010). Long-term stability of global erosion rates and weathering during late-Cenozoic cooling. *Nature*, *465*(7295), 211–214. https://doi.org/10.1038/nature09044

Wright, L. D., & Nittrouer, C. A. (1995). Dispersal of river sediments in coastal seas: Six contrasting cases. *Estuaries*, *18*(3), 494–508. https://doi.org/10.2307/1352367

Wurgaft, E., Steiner, Z., Luz, B., & Lazar, B. (2016). *Evidence for inorganic precipitation of CaCO3 on suspended solids in the open water of the Red Sea*. *Marine Chemistry* (Vol. 186). Elsevier B.V. https://doi.org/10.1016/j.marchem.2016.09.006

Yu, Z., Wang, X., Han, G., Liu, X., & Zhang, E. (2018). Organic and inorganic carbon and their stable isotopes in surface sediments of the Yellow River Estuary. *Scientific Reports*, *8*(1). https://doi.org/10.1038/s41598-018-29200-4

998 Zeng, S., Liu, Z., & Kaufmann, G. (2019). Sensitivity of the global carbonate weathering carbon-sink
999 flux to climate and land-use changes. *Nature Communications*, *10*(1), 1–10.
1000 https://doi.org/10.1038/s41467-019-13772-4

1001 Zhou, Y. Q., Sawyer, A. H., David, C. H., & Famiglietti, J. S. (2019). Fresh Submarine Groundwater
1002 Discharge to the Near-Global Coast. *Geophysical Research Letters*, *46*(11), 5855–5863.
1003 https://doi.org/10.1029/2019GL082749

1004